

This chapter contains the following copyrighted materials:

Reprinted Fig. 3 with permission from T. Nakamura et al., *Phys. Rev. Lett.* 96, 252502 (2006). Copyright 2006 by the American Physical Society.

Reprinted Fig. 4 with permission from T. Aumann et al., *Phys. Rev. C* 59, 1252 (1999). Copyright 1999 by the American Physical Society.

Reprinted Fig. 1 with permission from K. Miernik et al., *Phys. Rev. Lett.* 99, 192501 (2007). Copyright 2007 by the American Physical Society.

Reprinted Fig. 2 with permission from A. Spyrou et al., *Phys. Rev. Lett.* 108, 102501 (2012). Copyright 2012 by the American Physical Society.

Reprinted Fig. 3 with permission from I. Tanihata et al., *Phys. Rev. Lett.* 100, 192502 (2008). Copyright 2008 by the American Physical Society.

Reprinted Fig. 1 with permission from A. Ozawa et al., *Phys. Rev. Lett.* 84, 5493 (2000). Copyright 2000 by the American Physical Society.

Reprinted Fig. 2 with permission from I. Hamamoto, *Phys. Rev. C* 69, 041306(R) (2004). Copyright 2004 by the American Physical Society.

Reprinted Fig. 2 with permission from P. Adrich et al., *Phys. Rev. Lett.* 95, 132501 (2005). Copyright 2005 by the American Physical Society.

Readers may view, browse, and/or download material for temporary copying purposes only, provided these uses are for noncommercial personal purposes. Except as provided by law, this material may not be further reproduced, distributed, transmitted, modified, adapted, performed, displayed, published, or sold in whole or part, without prior written permission from the American Physical Society.

Reprinted Fig. 2 from *Phys. Lett.* B268, M. Fukuda et al., Neutron halo in ^{11}Be studied via reaction cross sections, p. 339 (1991), with permission from Elsevier.

Reprinted Fig. 3 from *Nucl. Phys.* A693, A. Ozawa, T. Suzuki, and I. Tanihata, Nuclear size and related topics, p. 32 (2001), with permission from Elsevier.

Reprinted Fig. 2 from *Phys. Lett.* B707, M. Takechi et al., Interaction cross sections for Ne isotopes towards the island of inversion and halo structures of ^{29}Ne and ^{31}Ne , p. 357 (2012), with permission from Elsevier.

Reprinted Fig. 3 from *Phys. Rep.* 264, T. Otsuka and N. Fukunishi, Nuclear mean field on and near the drip lines, p. 297 (1996), with permission from Elsevier.

Chapter 1

Exotic nuclei far from the stability line

K. Hagino¹, I. Tanihata^{2,3}, and H. Sagawa⁴

¹*Department of Physics, Tohoku University, Sendai 980-8578, Japan*

²*Research Center for Nuclear Physics (RCNP), Osaka University, Mihogaoka, Ibaraki, Osaka 5670047, Japan*

³*Research Center of Nuclear Science and Technology(RCNST) and School of Physics and Nuclear Energy Engineering, Beihang University, No. 37 Xueyuan Road, Haidian District, Beijing, P. R. China 100191*

⁴*Center for Mathematics and Physics, University of Aizu, Aizu-Wakamatsu, Fukushima 965-8560, Japan*

The recent availability of radioactive beams has opened up a new era in nuclear physics. The interactions and structure of exotic nuclei close to the drip lines have been studied extensively world wide, and it has been revealed that unstable nuclei, having weakly bound nucleons, exhibit characteristic features such as a halo structure and a soft dipole excitation. We here review the developments of the physics of unstable nuclei in the past few decades. The topics discussed in this Chapter include the halo and skin structures, the Coulomb breakup, the dineutron correlation, the pair transfer reactions, the two-nucleon radioactivity, the appearance of new magic numbers, and the pygmy dipole resonances.

1. Introduction

Until the middle of 1980's, nuclear physics had been developed by investigating primarily stable nuclei which exist in nature. Many facets of atomic nuclei had been revealed, which include a mass, density distribution, radius, shell structure, collective excitations, and various decay modes.¹⁻³ As a natural question, however, it had been discussed already in the late 1960's a question on how many neutrons can be bound for a given number of proton.⁴⁻⁶ The first international symposium on nuclei far from the stability line was held in 1966 at Lysekil, Sweden,⁷ followed by the succeeding conference held in 1970 at CERN.⁸ The questions which attracted nuclear physicists at that time include i) where is the neutron drip line? ii) do the nuclear models which were successful for stable nuclei work also for neutron-rich nuclei? and iii) the relevance to the r-process nucleosynthesis.⁴ It is remarkable that already in 1966 the ⁸He nucleus was predicted to be stable by about 10 MeV against a dissociation to ⁶He + 2n.⁹ The ¹¹Li nucleus was also predicted to be slightly

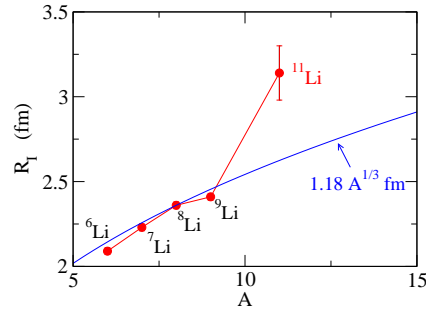


Fig. 1. The matter radii of Li isotopes deduced from the measured interaction cross sections with a carbon target at 790 MeV/nucleon. The solid line shows the systematics known for stable nuclei, $R \propto A^{1/3}$, where A is the mass number. The experimental data are taken from Ref. 10.

unbound, that is, only by 0.6 MeV, with respect to the ${}^9\text{Li}+2n$ configuration.⁹

The real start of the field of neutron-rich nuclei, however, was much later, that is, only in 1985, when an anomalously large matter radius of the ${}^{11}\text{Li}$ nucleus was experimentally discovered through the measurement of the interaction cross section.¹⁰ The matter radius was found to deviate largely from the known systematics in stable nuclei, which scales as $A^{1/3}$ as a function of mass number A of a nucleus (see Fig. 1). Together with a fact that the two-neutron separation energy, S_{2n} , is extremely small for this nucleus (S_{2n} was known to be 190 ± 110 keV at the time of 1985,¹¹ which has been updated to 378 ± 5 keV¹²), the large matter radius has been interpreted to be due to a long tail of the wave function for the weakly bound valence nucleons.¹³ This structure is referred to as *halo*, in which the density distribution of valence neutron(s) largely extends over the core nucleus. Since the proton and neutron density distributions are almost the same in stable nuclei, the discovery of the halo structure was a big surprise. Subsequently, the interpretation of the halo structure was supported also by the observed narrow momentum distribution of the ${}^9\text{Li}$ nucleus due to the breakup of ${}^{11}\text{Li}$.¹⁴ It has been recognized by now that this exotic structure is an important characteristic feature of neutron-rich nuclei, and it has attracted much attention.

The physics of neutron-rich nuclei has now been one of the main current subjects of nuclear physics. In fact, new generation RI beam facilities (such as RIBF at RIKEN in Japan,¹⁵ FAIR at GSI in Germany,¹⁶ SPIRAL2 at GANIL in France,¹⁷ and FRIB at MSU in the USA¹⁸) have been, or will soon be, in operation in the world wide. In this chapter, we summarize the developments of the physics of unstable nuclei in the past few decades. In Sec. II, we first discuss properties of one-neutron halo nuclei, that is, nuclei with a tightly bound core nucleus and a loosely bound valence neutron. We particularly discuss the role of single-particle angular momentum and the Coulomb dissociation. In Sec. III, we treat two-neutron halo nuclei. The main focus will be put on the correlation between the valence neutrons. As possible probes for the correlation, we discuss the Coulomb breakup,

the two-nucleon radioactivity, and the two-neutron transfer reactions. In Sec. IV, we consider heavier neutron-rich nuclei. The topics to be discussed include the matter radii and the neutron skin thickness, the odd-even staggering of interaction cross sections, alpha clustering, the shell evolution and the deformation, and the collective excitations such as the pygmy dipole resonances. Finally, we summarize the chapter in Sec. V.

As the physics of neutron-rich nuclei is diverse, it is almost impossible to cover all the topics in this chapter. We would like the readers to refer also to review articles,^{19–33} and references therein.

2. One-neutron halo nuclei

2.1. Role of single-particle angular momentum

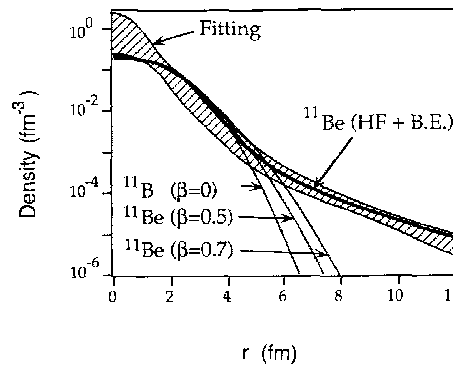


Fig. 2. The density distribution of the ^{11}Be nucleus which is consistent with the measured interaction cross sections (see the hatched area). Taken from Ref. 36.

We first discuss properties of one-neutron halo nuclei, for which a weakly-bound valence neutron moves around a core nucleus. A typical example is ^{11}Be , for which the interaction cross section has been found considerably large,^{10,34} similar to the ^{11}Li nucleus. The one neutron separation energy, S_n , is as small as 504 ± 6 keV,³⁵ which can be compared to the one neutron separation energy of *e.g.*, ^{13}C nucleus, $S_n=4.95$ MeV. This suggests that the ^{11}Be nucleus takes a halo structure. In fact, the large interaction cross section is consistent with a density distribution with a long tail, as has been shown in Ref. 36 (see Fig. 2).

It is instructive to consider a simple two-body model with a core nucleus plus a valence neutron in order to understand the halo phenomenon. That is, we solve the Schrödinger equation,

$$\left[-\frac{\hbar^2}{2m} \frac{d^2}{dr^2} + \frac{l(l+1)\hbar^2}{2mr^2} + V(r) - \epsilon_l \right] u_l(r) = 0, \quad (1)$$

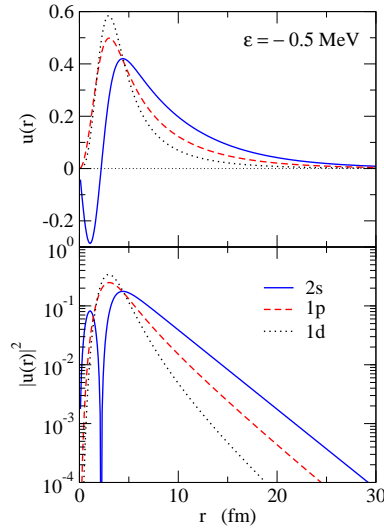


Fig. 3. The radial wave functions $u(r)$ for the relative motion between the valence neutron and the core nucleus ^{10}Be in the ^{11}Be nucleus. The upper panel shows the wave functions on the linear scale, while the lower panel shows the square of the wave functions on the logarithmic scale. The solid, the dashed, and the dotted lines correspond to the wave functions for the $2s$, $1p$, and $1d$ states, respectively. A Woods-Saxon shape is assumed for the mean-field potential, whose depth is adjusted for each angular momentum so that the single-particle energy is $\epsilon = -0.5$ MeV

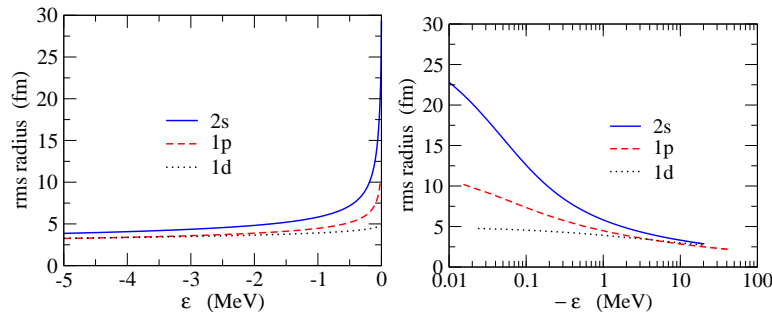


Fig. 4. The root-mean-square (rms) radii for the $2s$, $1p$, and $1d$ states in the ^{11}Be nucleus as a function of the single-particle energy ϵ . The meaning of each line is the same as in Fig. 3. The right panel is the same as the left panel, but plotted in the logarithmic scale for the horizontal axis.

where m is the nucleon mass, l is the single-particle angular momentum, and $V(r)$ is a spherical single-particle potential. Fig. 3 shows the radial wave function $u_l(r)$ on the linear (the upper panel) and the logarithmic (the lower panel) scales for the ^{11}Be nucleus with the two-body $^{10}\text{Be}+n$ model. We use a Woods-Saxon potential for $V(r)$ with the radius and the diffuseness parameters of $R=2.74$ fm and $a=0.75$ fm, respectively, whereas the depth parameter is adjusted for each angular momentum

l so that the single-particle energy ϵ is -0.5 MeV. For simplicity, we do not consider a spin-orbit interaction. The solid, the dashed, and the dotted lines show the wave functions for the $2s$, $1p$, and $1d$ states, respectively. One can clearly see that the wave function for the $2s$ state is largely extended, while that for the $1d$ state is spatially rather compact. The root-mean-square (rms) radii are 7.17, 5.17, and 4.15 fm for the $2s$, $1p$, and $1d$ states, respectively. Fig. 4 shows the rms radii as a function of the single-particle energy. As one can show analytically,³⁷ the rms radius diverges for $l = 0$ and 1 (it behaves as $|\epsilon|^{-1/2}$ for $l = 0$ and $|\epsilon|^{-1/4}$ for $l = 1$), while it converges to a constant value for higher values of l in the limit of zero binding energy. The halo structure, therefore, has been ascribed to an occupation of a weakly-bound $l = 0$ or $l = 1$ orbit by a valence nucleon near the threshold.^{37,38}

2.2. Coulomb dissociation

The halo structure significantly affects the dissociation process of a one-neutron halo nucleus in an external Coulomb field. The photoabsorption cross section for a dipole photon is given by

$$\sigma_\gamma = \frac{16\pi^3}{9\hbar c} E_\gamma \cdot \frac{dB(E1)}{dE_\gamma}, \quad (2)$$

where E_γ is the photon energy and

$$\frac{dB(E1)}{dE_\gamma} = \frac{1}{2j_i + 1} |\langle \psi_f || e_{E1} r Y_1 || \psi_i \rangle|^2 \delta(\epsilon_f - \epsilon_i - E_\gamma), \quad (3)$$

is the reduced transition probability (see *e.g.*, Appendix B of Ref. 3). Here, ψ_i and ψ_f denote the wave functions for the initial and the final states, respectively, j_i being the angular momentum for the initial state ψ_i . e_{E1} is the E1 effective charge, which is given by

$$e_{E1} = \frac{Z_1 A_2 - Z_2 A_1}{A_1 + A_2} e, \quad (4)$$

for a two-body system with a $(A_1, Z_1) + (A_2, Z_2)$ configuration.

A characteristic feature of the dipole excitation is that the $B(E1)$ distribution, $dB(E1)/dE$, has a strong peak in the low energy region when the binding energy is small (that is, the soft E1 mode^{13,39}). This large concentration of the E1 strength near the continuum threshold is caused by the optimal matching of wave functions between a weakly bound and continuum states. For a transition from an s -wave state to a p -wave state, the $B(E1)$ distribution can be evaluated analytically as

$$\frac{dB(E1)}{dE} = \frac{3\hbar^2}{\pi^2 \mu} e_{E1}^2 \frac{\sqrt{|E_b|} E_c^{3/2}}{(|E_b| + E_c)^4}, \quad (5)$$

if one employs a Yukawa function for ψ_i and a spherical Bessel function for the radial part of ψ_f ⁴⁰⁻⁴³ (see Refs. 44 and 45 for a general expression with arbitrary initial and final angular momenta). Here, μ is the reduced mass between the two

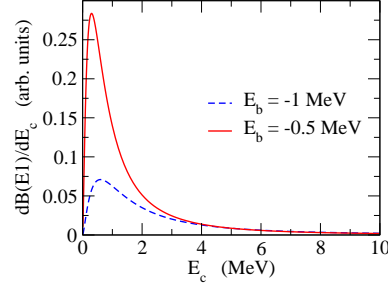


Fig. 5. The $B(E1)$ distribution from a bound s -wave state to continuum p -wave states given by Eq. (5) for two different values of the binding energy, E_b . It is plotted as a function of the relative energy of the final continuum state, E_c .

fragments, E_b is the energy of the initial bound state, and E_c is the energy of the final bound state, that is, the photon energy is $E_\gamma = E_c - E_b = E_c + |E_b|$. This equation indicates that the peak energy appears at $E_c = 3|E_b|/5$ with the height of the peak being proportional to $1/|E_b|^2$. The total strength is given by

$$B(E1) = \int dE \frac{dB(E1)}{dE} = \frac{3\hbar^2 e_{E1}^2}{16\pi^2 \mu |E_b|}. \quad (6)$$

Therefore, the peak position moves towards low energy as the binding energy, $|E_b|$, decreases, and at the same time the height of the peak increases, leading also to the increase of the total E1 strength. These features can be clearly seen in Fig. 5, which shows the $B(E1)$ distribution given by Eq. (5) for two different binding energies.

Notice that using Eq. (3) it is easy to derive that the total E1 strength (that is, the non-energy weighted sum rule) is proportional to the expectation value of r^2 with respect to the ground state,

$$B(E1) = \frac{3}{4\pi} e_{E1}^2 \langle r^2 \rangle_i. \quad (7)$$

As we mention in the previous subsection, the rms radius diverges in the zero binding limit for $l=0$ and 1 states, leading therefore to a divergence of the total E1 strength. Thus, an observation of a large E1 strength makes a clear indication of a halo structure of the nucleus.

Experimentally, the Coulomb dissociation of halo nuclei has been studied by Coulomb excitation experiments with a heavy target nucleus, such as ^{208}Pb .²⁸ The Coulomb breakup cross sections are often analyzed by the virtual photon theory, in which the cross sections are given as a product of the photo absorption cross sections, Eq. (2), and the virtual photon flux, $N_{E1}(E_\gamma)$.^{46,47} Figure 6 shows the experimental $B(E1)$ distribution for the ^{11}Be nucleus obtained by the Coulomb breakup reaction at 72 MeV/nucleon.⁴⁸ The observed dipole strength shows a strong peak at about 800 keV excitation energy, which is consistent with the binding energy of about

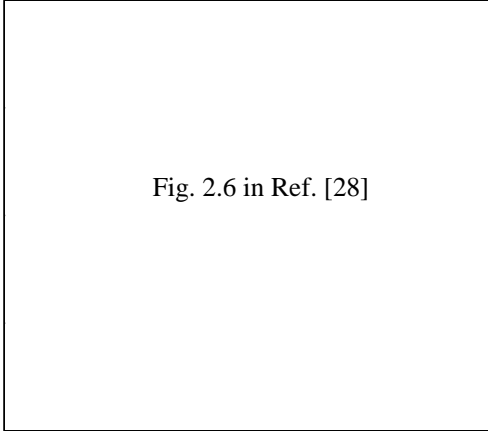


Fig. 2.6 in Ref. [28]

Fig. 6. The experimental $B(E1)$ distribution for the ^{11}Be nucleus deduced from the Coulomb breakup with a ^{208}Pb target at 70 MeV/nucleon.⁴⁸ Taken from Ref. 28.

500 keV. The peak is large, and is again consistent with the halo structure of this nucleus.

In addition to the large interaction cross sections,^{49,50} large Coulomb breakup cross sections are experimentally observed also for ^{19}C and ^{31}Ne .^{51,52} These nuclei are thus considered to be good candidates for halo nuclei.

3. Two-neutron halo nuclei

3.1. Two-nucleon correlation

Let us now discuss properties of two-neutron halo nuclei, in which two valence neutrons are weakly bound to a core nucleus. For these nuclei, one must consider a (pairing) interaction between the valence neutrons. It has been well recognized that the pairing correlation plays an important role in nuclear physics.^{3,53–55} It leads to an extra binding for even-mass nuclei, and at the same time reduces the level density in the low energy region. Also, a pairing interaction scatters nucleon pairs from a single-particle level below the Fermi surface to those above, and consequently each single-particle level is occupied only partially. For weakly bound nuclei, the pairing interaction works by scattering nucleon pairs inevitably to unbound states.

If one adopts a three-body model for a two-neutron halo nucleus, one could view it as a system of two interacting Fermions inside a confining potential. This is in a sense similar to a problem of interacting Fermion gas in a harmonic trap in atomic physics (see *e.g.*, Refs. 56 and 57, and references therein). But a problem is much more challenging in weakly bound nuclei, because a trapping potential is not an infinite well (in contrast to a harmonic trap) so that the couplings to continuum are important, and also because a trapping potential itself is constructed self-consistently from the interaction among nucleons.

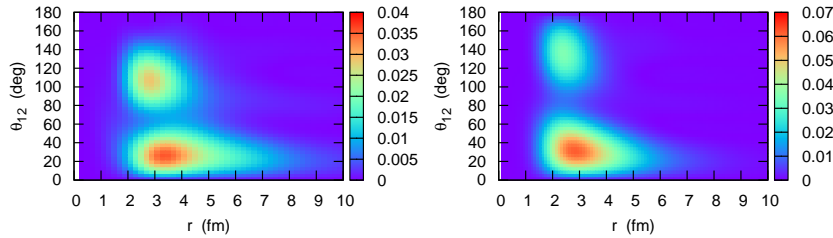


Fig. 7. The two-particle densities for ^{11}Li (the left panel) and for ^6He (the right panel) obtained with a three-body model calculation.⁶⁷ These are plotted as a function of neutron-core distance, $r_1 = r_2 \equiv r$, and the opening angle between the valence neutrons, θ_{12} . The densities are weighted with a factor $8\pi^2 r^4 \sin \theta_{12}$.

Among two-neutron halo nuclei, the so called Borromean nuclei have attracted lots of attention. These are unique three-body bound systems, in which any two-body subsystem is not bound.^{58,59} Typical examples include ^{11}Li and ^6He , which can be viewed as three-body systems consisting of a core nucleus and two valence neutrons. Since both the n - n and n -core two-body subsystems are not bound, these nuclei are bound only as three-body systems.

One of the most important current open questions concerning the Borromean nuclei is to clarify the characteristic nature of correlations between the two valence neutrons, which do not form a bound state in the vacuum. For instance, a spatial structure of two valence neutrons in the Borromean nuclei has attracted much attention. As a matter of fact, this has a long history of research as a general problem in nuclear physics. One of the oldest publications on this problem is by Bertsch, Broglia, and Riedel, who solved a shell model for ^{210}Pb and showed that the two valence neutrons are strongly clusterized.⁶⁰ Subsequently, Migdal argued that two neutrons may be bound in a nucleus even though they are not bound in the vacuum.⁶¹ The strong localization of two neutrons inside a nucleus has been referred to as *dineutron correlation*. It has been shown in Ref. 62 that the dineutron correlation is caused by admixtures of a few single-particle orbits with opposite parity.

Although the dineutron correlation exists even in stable nuclei,^{63–65} it is enhanced in weakly bound nuclei because the admixtures of single-particle orbits with different parities are easier due to the couplings to the continuum spectra. Probably it was Hansen and Jonson who exploited the idea of dineutron correlation explicitly for exotic nuclei for the first time. They proposed the dineutron cluster model and successfully analyzed the matter radius of ^{11}Li .¹³ They also predicted a large Coulomb dissociation cross section of the ^{11}Li nucleus. In the 1990's, more microscopic three-body model calculations for neutron-rich nuclei started.^{58,59} These three-body model calculations have revealed that a strong dineutron correlation, where the two valence neutrons take a spatially compact configuration, indeed ex-

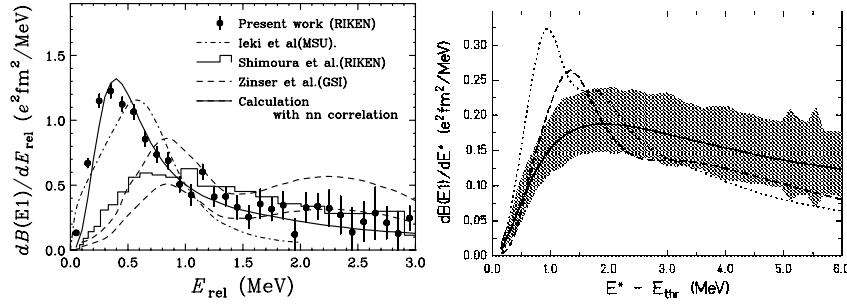


Fig. 8. The experimental B(E1) distributions for the ^{11}Li (the left panel) and for the ^6He (the right panel) nuclei deduced from the Coulomb breakup measurements. Taken from Refs. 79 and 80.

ists in weakly-bound Borromean nuclei.^{27,58,59,66–69} It has been shown that the dineutron correlation exists also in heavier neutron-rich nuclei^{64,70–74} as well as in infinite neutron matter.^{75–77} The diproton correlation, which is a counter part of the dineutron correlation, has also been shown to exist in the proton-rich Borromean nucleus, ^{17}Ne .⁷⁸

Figs. 7(a) and 7(b) show the two-particle density obtained with three-body model calculations for ^{11}Li and ^6He , respectively. These are plotted as a function of the neutron-core distance, $r_1 = r_2 \equiv r$ and the opening angle between the valence neutrons, θ_{12} . A weight of $4\pi r^2 \cdot 2\pi r^2 \sin \theta_{12}$ has been multiplied. See Ref. 67 for the details of the calculations. One can see that a large fraction of two-particle density is concentrated in the region with small opening angle θ_{12} for both the nuclei. This is a clear manifestation of the strong dineutron correlation discussed in this subsection.

3.2. Coulomb breakup

The Coulomb breakup of two-neutron halo nuclei can be discussed in a similar manner as that of one-neutron halo nuclei discussed in Sec. 2.2. The only difference is that the E1 operator is now given by

$$\hat{D}_\mu = e_{\text{E1}} R Y_{1\mu}(\hat{\mathbf{R}}), \quad (8)$$

where

$$\mathbf{R} = \frac{\mathbf{r}_1 + \mathbf{r}_2}{2}, \quad (9)$$

is the center of mass coordinate for the two valence neutrons, and the E1 effective charge is given by

$$e_{\text{E1}} = \frac{2Z_c}{A_c + 2} e, \quad (10)$$

with A_c and Z_c being the mass and charge numbers for the core nucleus.

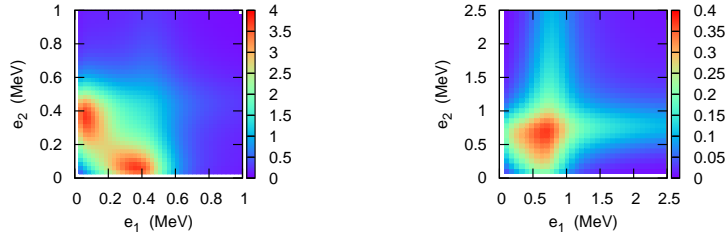


Fig. 9. The dipole strength distribution, $d^2B(E1)/de_1de_2$, of ^{11}Li (the left panel) and ^6He (the right panel) as a function of the energies of the two emitted neutrons relative to the core nucleus. It is plotted in units of $\text{e}^2\text{fm}^2/\text{MeV}^2$. See Ref. 82 for the details of the calculations.

The left and the right panels of Fig. 8 show the measured $B(E1)$ distribution for the ^{11}Li and ^6He nuclei,^{79,80} respectively. Those $B(E1)$ distributions, especially that for the ^{11}Li nucleus, show a strong concentration in the low excitation region, similar to the $B(E1)$ distribution for the ^{11}Be nucleus shown in Fig. 6, reflecting the halo structure of these nuclei. Moreover, the experimental data for ^{11}Li are consistent with the theoretical calculation only when the interaction between the valence neutrons is taken into account, strongly suggesting the existence of the dineutron correlation in this nucleus (see also Ref. 81).

The left and the right panels of Fig. 9 show calculated dipole strength distributions, $d^2B(E1)/de_1de_2$, of ^{11}Li and ^6He , respectively, obtained with the three-body model⁸² together with the Green's function method for the continuum dipole response.⁸³ Here, e_1 (e_2) is the relative energy between the first (second) neutron and the core nucleus. One immediately notices that the strength distribution is considerably different between ^{11}Li and ^6He , despite similar ground state density to each other (see Fig. 7). This difference has been shown to be due to the different resonance properties of the neutron-core interaction between the two nuclei⁸² (see also Ref. 69).

3.3. Charge radii of halo nuclei

Until recently Na was the lightest element of which charge radii (or proton density distribution radii) of neutron-rich short lived isotopes have been measured. Combined with the measurements of matter radii, the development of neutron skins thus has been presented for Na isotopes.⁸⁴ For neutron halo nuclei, interaction cross section and fragmentation measurements have provided a mean to determine the matter density distribution. However the proton density distribution could not be determined directly from such measurements. Although the proton distribution has been considered not to extend out even when neutron halos are formed, based on the fact that narrow momentum distributions, that indicate long tails of distribution, are observed only for a neutron or two-neutron removal channels of

fragmentation, no direct determination of proton distribution radii (or charge radii) was possible until recently.

Recent developments of ion traps now provide a means to determine charge radii of very light neutron rich nuclei including neutron halo nuclei, ${}^6\text{He}$, ${}^{11}\text{Li}$, and ${}^{11}\text{Be}$. The charge radii are determined by the isotope shift measurements of atomic transitions. In a very light atom, the isotope shift $\delta\nu$ includes two terms,

$$\delta\nu = \delta\nu_{\text{MS}} + \delta\nu_{\text{FS}}. \quad (11)$$

The first term $\delta\nu_{\text{MS}}$ is the mass shift that is proportional to the difference of the masses (A and A') of two isotopes,

$$\delta\nu_{\text{MS}} \propto \frac{A - A'}{AA'}, \quad (12)$$

and $\delta\nu_{\text{FS}}$ is the field shift which is proportional to the difference of the rms radii of nuclei,

$$\delta\nu_{\text{FS}} \propto Z \times \Delta[\Psi(0)]^2 \times \delta\langle r^2 \rangle, \quad (13)$$

where Z is the atomic number of the isotopes and $\Delta[\Psi(0)]^2$ is the difference of the electron wave function at the nuclei. To obtain the field shift, the mass shift has to be calculated theoretically and then subtracted from the total isotope shift determined from the measurement.

For a light nucleus as an example, the mass shift term for ${}^6\text{He}$ and ${}^4\text{He}$ is more than 10^5 times larger than the shift expected from a change of radius. The mass shift term cannot be separately measured experimentally so that an accurate theoretical estimation of this term is necessary in order to determine the charge radii. The recent development of atomic theory of a few electron system has enabled to do such a calculations successfully up to three electron systems.⁸⁵

The charge radii of ${}^6\text{He}$ and ${}^8\text{He}$ have been determined by the ANL group using ANL/ATLAS and GANIL RIB facilities to be 2.054 ± 0.014 fm and 1.93 ± 0.03 fm, respectively.^{86,87} Those experiments use a magneto-optical trap of atoms for precision laser spectroscopy. The charge radii of Li and Be isotopes are determined by a GSI group using TRIUMF/ISAC facility and ISOLDE RIB facilities.^{88,89} In these experiments, a Doppler-free two-photon transition was used for the lithium measurements^{88,90,91} and collinear laser spectroscopy with a frequency comb for the beryllium isotopes.⁸⁹

The proton distribution rms radii, $R_p \equiv \sqrt{\langle r_p^2 \rangle}$, has been calculated from the charge radii, $\sqrt{\langle r_{ch}^2 \rangle}$, by,

$$\langle r_{ch}^2 \rangle = \langle r_p^2 \rangle + \langle \rho_p^2 \rangle + \frac{N}{Z} \langle \rho_n^2 \rangle + \frac{3\hbar^2}{4m_p^2 c^2}, \quad (14)$$

where r_p is the radius of point proton distribution of a nucleus, ρ_p and ρ_n are the charge radii of free proton and free neutron, $\langle \rho_p^2 \rangle = 0.769 \pm 0.012$ and $\langle \rho_n^2 \rangle =$

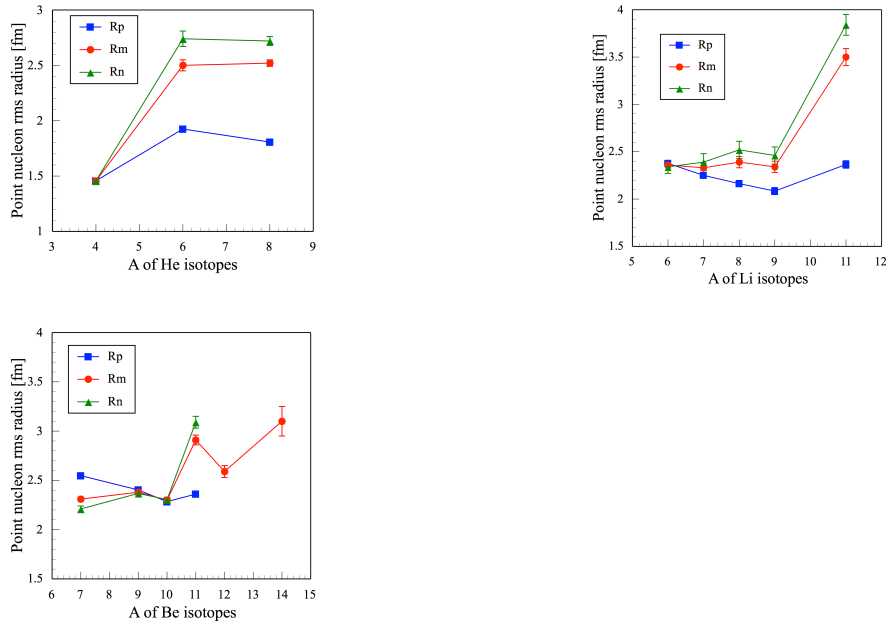


Fig. 10. The matter, proton, and neutron rms radii (R_m , R_p , and R_n) for He, Li, and Be isotopes determined from the interaction/reaction cross section and the charge radius measurements.

$-0.1161 \pm 0.0022 \text{ fm}^2$,⁹² and the last term is the so called Darwin-Foldy term (0.033 fm^2).⁹³ The relation between matter, proton, and neutron rms radii is written as,

$$AR_m^2 = ZR_p^2 + NR_n^2. \quad (15)$$

The rms radii of matter (or point nucleon distribution), R_m , have been determined by the interaction cross section and reaction cross section measurements.⁸⁴ The matter (R_m), proton (R_p), and neutron (R_n) radii so determined are presented in Fig. 10 for He, Li, and Be isotopes. One can clearly see that R_p is much smaller than that of neutron R_n in neutron rich isotopes and in particular in halo nuclei. However the proton radius increases slightly when neutron halo is formed. This observation is consistent with the view of a core+decoupled halo neutron(s) structure of halo nuclei that has been widely used for modeling halo nuclei. Under this model, the core of a halo nucleus has the same proton distribution as the isolated core nucleus. Because of the large distance between the core and the halo neutron(s), the core moves around the center of mass of the halo nucleus and therefore the proton radius in a halo nucleus is larger than that of isolated core.

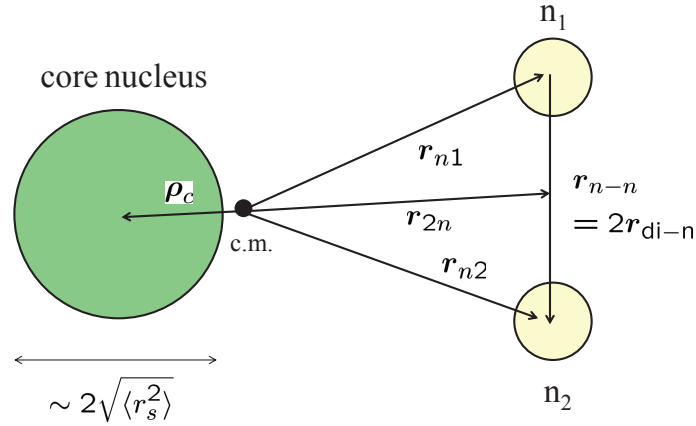


Fig. 11. The geometry of the three-body model for two-neutron halo nuclei.

3.4. Geometry of two-neutron halo nuclei

Under the assumption of core+ two-neutron for a two-neutron halo nucleus, the spatial correlation of halo neutrons can be studied. The geometry of the model for such a nucleus is shown in Fig. 11.

The relation between nucleon, proton, and neutron mean-square (ms) radii for a nucleus i is given by a similar equation as Eq. (15). Therefore from the measurements of matter and charge radii of a halo nucleus and its core nucleus, all radii of the halo nucleus, $\langle r_m^2 \rangle$, $\langle r_p^2 \rangle$, and $\langle r_n^2 \rangle$, and the core, $\langle r_{sm}^2 \rangle$, $\langle r_{sp}^2 \rangle$, and $\langle r_{sn}^2 \rangle$, are determined. One can also define the ms matter radii of the halo neutrons, $\langle r_h^2 \rangle$, and that of the core, $\langle r_{cm}^2 \rangle$, which are related as,

$$A\langle r_m^2 \rangle = A_c\langle r_{cm}^2 \rangle + A_h\langle r_h^2 \rangle, \quad (16)$$

where A , A_c , and A_h are the mass numbers of the halo nucleus, the core nucleus, and the number of halo neutrons, respectively.

Using the coordinate of the core nucleus, ρ_c , relative to the center of mass of the halo nucleus, that is, the movement of the center of the core in the halo nucleus, the relation between the nucleon, proton, and neutron radii between the core and the halo nucleus are represented as,

$$\langle r_{cp}^2 \rangle = \langle r_p^2 \rangle = \langle r_{sp}^2 \rangle + \langle \rho_c^2 \rangle, \quad (17)$$

$$\langle r_{cm}^2 \rangle = \langle r_{sm}^2 \rangle + \langle \rho_c^2 \rangle, \quad (18)$$

$$\langle r_{cn}^2 \rangle = \langle r_{sn}^2 \rangle + \langle \rho_c^2 \rangle, \quad (19)$$

From those equations, one can obtain the movement of the core, $\langle \rho_c^2 \rangle$. Then the ms radius of the halo distribution, $\langle r_h^2 \rangle$, is also determined from Eq. (16).

The distance between the center of mass of the halo nucleus and the center of mass of the two halo neutrons (r_{2n}) can be calculated from ρ_c ,

$$A_h^2 \langle r_{2n}^2 \rangle = A_c^2 \langle \rho_c^2 \rangle. \quad (20)$$

The distance between the core and the two-neutron center of mass is $\sqrt{\langle r_{c-2n}^2 \rangle} = \sqrt{\langle r_{2n}^2 \rangle} + \sqrt{\langle \rho_c^2 \rangle}$. Let us define the size of di-neutron as the distribution radius of the neutrons around the center of mass of halo neutrons, $\mathbf{r}_{n-n} = \mathbf{r}_{n1} - \mathbf{r}_{n2} = 2\mathbf{r}_{di-n}$, and thus $r_{n-n}^2 = 4r_{di-n}^2$, that is, r_{di-n} is the radius of the di-neutron forming the halo. The radius of the halo distribution in the halo nucleus and the dineutron radius is related as,

$$\langle r_h^2 \rangle = \langle r_{2n}^2 \rangle + \langle r_{di-n}^2 \rangle. \quad (21)$$

Using these $\langle r_h^2 \rangle$ and $\langle r_{2n}^2 \rangle$, one can determine the di-neutron ms radius and thus the ms separation distance $\langle r_{n-n}^2 \rangle$ of the two halo neutrons. Notice that combining Eqs. (16), (18), (20), and (21) yields

$$\langle r_m^2 \rangle = \frac{A_c}{A_c + 2} \langle r_{sm}^2 \rangle + \frac{1}{A_c + 2} \left(\frac{2A_c}{A_c + 2} \langle r_{c-2n}^2 \rangle + \frac{1}{2} \langle r_{n-n}^2 \rangle \right), \quad (22)$$

for $A_h = 2$.

One can also obtain the two-neutron cross term $\langle \mathbf{r}_{n1} \cdot \mathbf{r}_{n2} \rangle$ as

$$\langle \mathbf{r}_{n1} \cdot \mathbf{r}_{n2} \rangle = \frac{1}{4} (A_c^2 \langle \rho_c^2 \rangle - \langle r_{n-n}^2 \rangle), \quad (23)$$

from

$$A_c^2 \langle \rho_c^2 \rangle = \langle (\mathbf{r}_{n1} + \mathbf{r}_{n2})^2 \rangle, \quad \text{and} \quad \langle r_{n-n}^2 \rangle = \langle (\mathbf{r}_{n1} - \mathbf{r}_{n2})^2 \rangle, \quad (24)$$

where $A_h = 2$ has been used.

The empirical values for those variables for ${}^6\text{He}$ and ${}^{11}\text{Li}$, extracted from the experimental interaction cross sections and charge radii, are shown in Table 1 and 2. Corresponding theoretical values are also shown in the tables for a few model calculations. The data for ${}^6\text{He}$ and ${}^{11}\text{Li}$ show that the distance between the core and the halo neutrons, $\sqrt{\langle r_{c-2n}^2 \rangle}$, is almost equal to the distance between two neutrons, $\sqrt{\langle r_{n-n}^2 \rangle}$, indicating that two-neutrons are sitting close together and have strong *di-neutron* correlations. The opening angle between the valence neutrons with respect to the core nucleus can be calculated from the empirical values for $\sqrt{\langle r_{c-2n}^2 \rangle}$ and $\sqrt{\langle r_{n-n}^2 \rangle}$ to be $\langle \theta_{12} \rangle = 58.9 \pm 12.6$ and $\langle \theta_{12} \rangle = 54.2 \pm 3.04$ degrees for ${}^{11}\text{Li}$ and ${}^6\text{He}$, respectively. (We should remark here that it is misleading to say that two neutrons are mostly sitting with opening angles obtained in this way. Instead, the mean opening angle is an average of a smaller and a larger correlation angles in the density distribution shown in Fig. 7.)

Table 1. The root-mean-square (rms) radii of ${}^6\text{He}$. $\sqrt{\langle r_m^2 \rangle}$, $\sqrt{\langle r_p^2 \rangle}$, and $\sqrt{\langle r_n^2 \rangle}$ are the point nucleon, proton, and neutron rms radii of the nucleus, respectively. $\sqrt{\langle r_h^2 \rangle}$ is the rms radius of the halo-neutron distribution. $\sqrt{\langle r_{2n}^2 \rangle}$ is the rms distance from the center of mass of the nucleus to the center of mass of the two valence neutrons, while $\sqrt{\langle r_{c-2n}^2 \rangle}$ is the rms distance from the ${}^4\text{He}$ core to the center of mass of the two valence neutrons. The first estimation for the latter quantity by Wang *et al.* was 3.71 ± 0.07 fm.⁸⁶ $\sqrt{\langle r_{n-n}^2 \rangle}$ is the rms distance between the valence neutrons, while $\langle \mathbf{r}_{n1} \cdot \mathbf{r}_{n2} \rangle$ is the correlation of the two valence neutrons. All these radii are given in the unit of fm, except for $\langle \mathbf{r}_{n1} \cdot \mathbf{r}_{n2} \rangle$, which is given in the unit of fm². See text for explanation. GFMC, NCSM, and AMD denote Greens Function Monte Carlo, No-Core Shell Model, and Anti-symmetrized Molecular Dynamics, respectively.

	Experiment	GFMC ⁸¹	Varga ⁹⁴	Esbensen ⁹⁵	Funada ⁹⁶	Zhukov ⁵⁹	NCSM ⁹⁷	AMD ⁹⁸
$\sqrt{\langle r_m^2 \rangle}$	2.43 ± 0.03		2.46			2.45		2.23
$\sqrt{\langle r_p^2 \rangle}$	1.912 ± 0.018		1.80				1.89 ± 0.04	1.83
$\sqrt{\langle r_n^2 \rangle}$	2.65 ± 0.04		2.67				2.67 ± 0.05	2.40
$\sqrt{\langle r_n^2 \rangle} - \sqrt{\langle r_p^2 \rangle}$	0.808 ± 0.047		0.87					
$\sqrt{\langle r_h^2 \rangle}$	3.37 ± 0.11							
$\sqrt{\langle r_{2n}^2 \rangle}$	2.52 ± 0.05		3.42					
$\sqrt{\langle r_{c-2n}^2 \rangle}$	3.84 ± 0.06	3.81 ± 0.20		3.63	3.51	3.54		
$\sqrt{\langle r_{n-n}^2 \rangle}$	3.93 ± 0.25			4.62	4.55	4.58		
$\langle \mathbf{r}_{n1} \cdot \mathbf{r}_{n2} \rangle$ (fm ²)	2.70 ± 0.97			0.54	0.292	0.325		

Table 2. Same as Table I, but for ${}^{11}\text{Li}$. The first estimation of $\sqrt{\langle r_{c-2n}^2 \rangle}$ by Sanchez *et al.* was 6.2 ± 0.3 fm.⁸⁸ SHF and TOSM denote Skyrme Hartree-Fock and Tensor Optimized Shell Model, respectively.

	Experiment	Esbensen ⁹⁵	SHF ⁹⁹	Zhukov ⁵⁹	TOSM ¹⁰⁰
$\sqrt{\langle r_m^2 \rangle}$	3.50 ± 0.09		2.87	3.39	3.41
$\sqrt{\langle r_p^2 \rangle}$	2.37 ± 0.04		2.28		2.34
$\sqrt{\langle r_n^2 \rangle}$	3.84 ± 0.11		3.06		3.73
$\sqrt{\langle r_n^2 \rangle} - \sqrt{\langle r_p^2 \rangle}$	1.48 ± 0.12				
$\sqrt{\langle r_h^2 \rangle}$	6.1 ± 0.3				
$\sqrt{\langle r_{2n}^2 \rangle}$	5.0 ± 0.5				
$\sqrt{\langle r_{c-2n}^2 \rangle}$	6.2 ± 0.5	5.12	6.26	5.69	
$\sqrt{\langle r_{n-n}^2 \rangle}$	7.0 ± 1.7	6.77			7.33
$\langle \mathbf{r}_{n1} \cdot \mathbf{r}_{n2} \rangle$ (fm ²)	2.70 ± 0.97				

In principle, a similar analysis can be made for ${}^8\text{He}$. However it is known that the possible core ${}^6\text{He}$ is known not to be a good inert core and thus ${}^6\text{He} + 2n$ model is very poor. Instead, it is known from the fragmentation experiment¹⁰¹ that ${}^4\text{He} + 4n$ is a good model of ${}^8\text{He}$ ground state. Following the similar procedure as above, one can determine the movement of the 4-valence neutron center-of-mass in ${}^8\text{He}$, $\sqrt{\langle r_{4n}^2 \rangle}$ to be 1.07 ± 0.05 fm. This value is much smaller than that in ${}^6\text{He}$, $\sqrt{\langle r_{2n}^2 \rangle}/2 = 1.62 \pm 0.03$ fm. It is an indication that the four neutrons in ${}^8\text{He}$ are distributed more uniformly than in ${}^6\text{He}$.

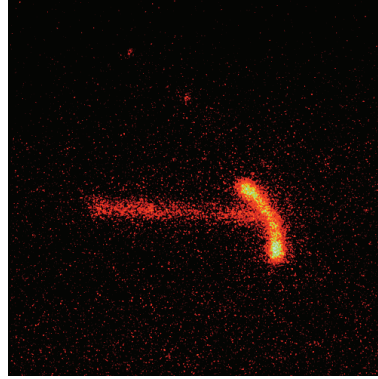


Fig. 12. An example of trajectories of the two emitted protons from the two-proton radioactivity of ^{45}Fe recorded by a CCD camera. Taken from Ref. 114.

Notice that the core-2n rms distance, $\sqrt{\langle R^2 \rangle} = \sqrt{\langle r_{c-2n}^2 \rangle}$, for two-neutron halo nuclei can be estimated also from the Coulomb dissociation cross sections. For the transition operator given by Eq. (8), the expectation value of R^2 in the ground state can be estimated from the total $B(\text{E1})$ value as

$$B_{\text{tot}}(\text{E1}) \sim \frac{3}{\pi} \left(\frac{Z_c e}{A_c + 2} \right)^2 \langle R^2 \rangle, \quad (25)$$

(see also Eq. (7)). Using the experimental matter radii to estimate the rms distance $\sqrt{\langle r_{n-n}^2 \rangle}$, the opening angle between the valence neutrons with respect to the core nucleus has been extracted as¹⁰² $\langle \theta_{12} \rangle = 65.2 \pm 12.2$ degrees for ^{11}Li and 74.5 ± 12.1 degrees for ^6He (see also Ref. 103), which agree well with the results of the three-body model calculation of Ref. 67. The value of $\langle \theta_{12} \rangle$ for ^{11}Li is consistent also with the one obtained in Table 1 and 2, although the value for ^6He is somewhat larger.

3.5. Two-nucleon radioactivity

Although the experimental observation of the strong low-lying dipole strength distribution in the ^{11}Li nucleus (see Fig. 8) has provided an experimental signature of the existence of dineutron correlation in this nucleus, it is still an open question how to probe it directly. That is, in the Coulomb breakup process, the ground state wave function of a two-neutron halo nucleus is perturbed by the external electromagnetic field of the target nucleus, and it may not be easy to disentangle the dineutron correlation in the ground state from that in the excited states. It would be desirable if one could find an observable which reflects only the properties of the ground state.

The two-proton radioactivity, that is, a spontaneous emission of two valence protons, of proton-rich nuclei^{29,104–107} is expected to provide a good tool to probe

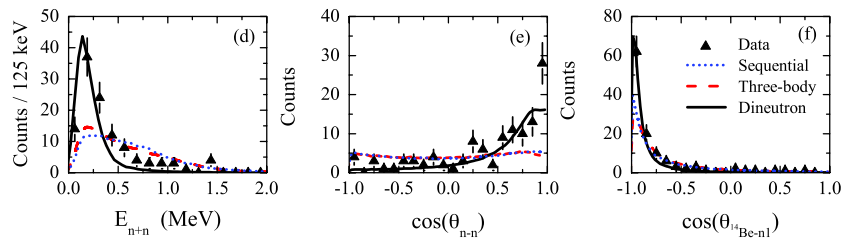


Fig. 13. The energy and the angular distributions of the two emitted neutrons from the two-neutron radioactivity of ^{16}Be . Taken from Ref. 116.

the di-proton correlation in the initial wave function. Nuclei beyond the proton drip line are unstable against proton emission, but, since a proton has to penetrate the Coulomb barrier, their lifetime is sufficiently long to study their spectroscopic properties. A single-proton radioactivity has been found in many odd- Z proton-rich nuclei, and has provided a powerful tool to study the spectroscopy of proton-rich nuclei beyond the proton-drip line.^{29,104,108–110} When the single-proton emission is energetically forbidden, proton-rich nuclei beyond the proton drip line decay via emission of two protons. Even though this process had been predicted theoretically in 1960,¹¹¹ its first experimental discovery was much later, only in 2002,^{112,113} for the ^{45}Fe nucleus. Subsequently, the energy and the angular distributions of the two emitted protons were also measured.¹¹⁴ An impressive development in Ref. 114 was the use of a new type of a gaseous detector, in which images of ionizing particle trajectories can be optically recorded with a CCD camera. An example of recorded trajectories of the two emitted protons from the two-proton radioactivity of ^{54}Fe is shown in Fig. 12. This technique was used also for the two-proton radioactivity of ^{48}Ni .¹¹⁵

Very recently, a ground state *two-neutron* emission was discovered for the first time for ^{16}Be .¹¹⁶ This is an analogous process of the two-proton radioactivity, corresponding to a penetration of two neutrons over a centrifugal barrier. For the ^{16}Be nucleus, the one-neutron emission process is energetically forbidden, which makes ^{16}Be an ideal two-neutron emitter. It is remarkable that the observed energy and the angular distributions of the two emitted neutrons show a strong indication of the dineutron correlation in the ground state of ^{16}Be (see Fig. 13).¹¹⁶

3.6. Two-neutron transfer reactions

It has been recognized for a long time that two-neutron transfer reactions are sensitive to the pairing correlation.^{117–120} The probability for the two-neutron transfer process is enhanced as compared to a naive expectation of sequential transfer process, that is, the square of one-neutron transfer probability.^{121,122} The enhancement of pair transfer probability has been attributed to the pairing effect, such as the enhancement of pair strength function^{123,124} and the surface localization of a Cooper pair.^{62,125} The pair transfer reaction is thus considered to provide a promising way

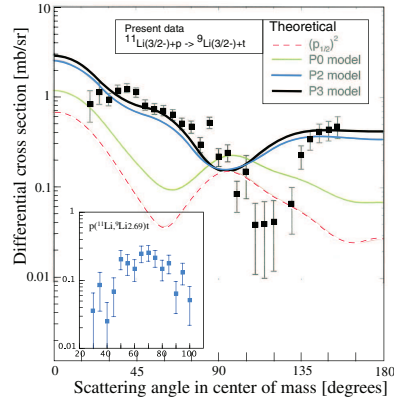


Fig. 14. The experimental angular distributions for the ${}^1\text{H}({}^{11}\text{Li}, {}^9\text{Li}){}^3\text{H}$ reaction at 3 MeV/nucleon. Taken from Ref. 132.

to probe the dineutron correlation discussed in Sec. 3.1. However, the reaction dynamics is rather complicated and has not even been well established. For instance, it is only in a recent calculation that a theoretical calculation achieves a satisfactory agreement with the experimental data.¹²⁶ It would therefore be not surprising that the role of dineutron in the pair transfer reaction has not yet been fully clarified.

One example is a relative importance of the one-step (the simultaneous pair transfer) process and the two-step (the sequential pair transfer) process. In heavy-ion pair transfer reactions of stable nuclei, both processes are known to play a role.^{127–129} For weakly-bound nuclei, most of the intermediate states for the two-step process are likely in the continuum spectra. It is still an open question how this fact, together with the Q -value matching condition,¹³⁰ alters the dynamics of the pair transfer reaction of neutron-rich nuclei.¹³¹

On the other hand, the cross sections for the pair transfer reaction of the Borromean nuclei, ${}^{11}\text{Li}$ and ${}^6\text{He}$, have been measured recently.^{132–137} The data for the ${}^1\text{H}({}^{11}\text{Li}, {}^9\text{Li}){}^3\text{H}$ reaction at 3 MeV/nucleon indicate that the cross sections are indeed sensitive to the pair correlation in the ground state of ${}^{11}\text{Li}$ (see Fig. 14).¹³² That is, the experimental cross sections can be accounted for only when the s -wave component is mixed in the ground state of ${}^{11}\text{Li}$ by 30-50%. Another important finding in this measurement is that significant cross sections were observed for the pair transfer process to the first excited state of ${}^9\text{Li}$,¹³² which has made a good support for the idea of phonon mediated pairing mechanism.¹³⁸

The two-neutron transfer from ${}^6\text{He}$ was investigated using ${}^4\text{He}$ and p targets at FLNR(Dubna) at 151 MeV.^{133,134} The angular distribution from the ${}^4\text{He}({}^6\text{He}, {}^4\text{He}){}^6\text{He}$ reaction shows dominant contribution from di-neutron configuration (see the dashed line in Fig. 15 (a)). While the wavefunction contains both the cigar and di-neutron correlation the amplitude of the latter is larger (Fig.15 (b), see also Fig. 7). The elastic scattering ${}^4\text{He}({}^6\text{He}, {}^6\text{He}){}^4\text{He}$ was also studied at center

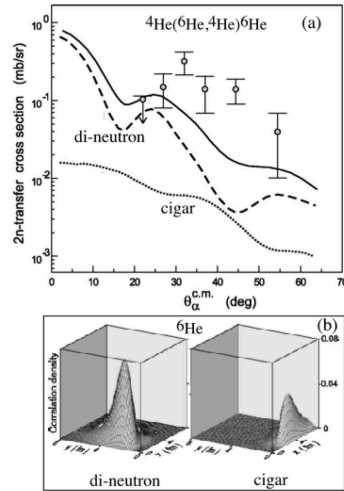


Fig. 15. (a) The angular distribution of the two-neutron transfer in the ${}^4\text{He}({}^6\text{He}, {}^4\text{He}){}^6\text{He}$ reaction.¹³⁴ The dashed line shows the calculation considering the dineutron component of the wave function while the dotted line is that with the cigar component. (b) The correlation densities in the wave function of ${}^6\text{He}$ for the dineutron and the cigar components.

of mass energies of 11.6 MeV and 15.9 MeV at the ARENAS facility at Louvain-La-Neuve.¹³⁵ An interpretation of the data at both energies^{133,135} showed that the rise of cross section at large angle were due to two-neutron transfer. The calculation was carried out based on the coupled reaction channels approach¹³⁹ including both one-step and sequential two-step transfer with realistic form factors. It was further found¹³⁹ that the direct two-neutron transfer strongly dominates over the sequential transfer at the low energies where the minimum in the angular distribution^{135,139} is due to direct 2n transfer. The sequential transfer becomes more sizable for the higher-energy data, though direct 2n transfer still dominates. In the analysis in Ref. 139, ${}^6\text{He}$ was modeled as core +2n bound state wavefunction where two $p_{3/2}$ neutrons coupled to $J=0$ (S-wave) and 1 (P-wave). The direct two-neutron transfer was found to be mainly due to the contribution from the S-wave. The P-wave part of the wave function belongs to the cigar type configuration, which is found to be a smaller contribution. The main conclusion is thus the same as Ref. 133, and the dominance of S-wave two-neutron cluster transfer shows strongly correlated two neutrons in ${}^6\text{He}$.

The $p({}^6\text{He}, {}^4\text{He})t$ angular distribution¹³³ (Fig. 16) when compared with the ${}^6\text{Li}(p, {}^3\text{He}){}^4\text{He}$, shows a slightly larger cross section for 2n transfer at the center-of-mass (cm) scattering angles near 60 degrees. This was interpreted to be a signature of a more disperse 2n wavefunction in ${}^6\text{He}$ compared to the compact d in ${}^6\text{Li}$. In both reactions a direct 2n transfer was assumed to be the dominant process. The $p({}^6\text{He}, t)$ reaction was also studied at 25 MeV/nucleon at GANIL,¹³⁶ with an aim

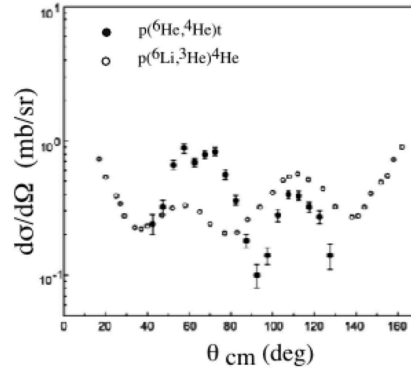


Fig. 16. The angular distributions for $p(^6\text{He},^4\text{He})t$ (the filled circles) and $p(^6\text{Li},^3\text{He})^4\text{He}$ (the open circles).¹³⁶

at looking into possible $t+t$ cluster existing in ^6He beside the interest in exploring the $^4\text{He}+2n$ configuration. The data are closer in magnitude and shape to the $2n$ transfer than the transfer of tritons. Therefore, the $^4\text{He}+2n$ configuration of ^6He is again confirmed.

In the experiment with a heavier target, that is, the $^6\text{He}+^{65}\text{Cu}$ reaction at $E_{\text{lab}}=22.6$ MeV, both the 1-neutron ($1n$) and the 2-neutron ($2n$) transfer cross sections were measured.¹³⁷ An interesting observation for this system is that the cross sections for the $2n$ transfer are much larger than those for the $1n$ transfer.¹³⁷ For stable nuclei, usually the $1n$ transfer cross sections are much larger than the $2n$ transfer cross sections,¹¹⁸ and the opposite observation for the $^6\text{He}+^{65}\text{Cu}$ system can be regarded as a characteristic feature of a Borromean nucleus. A similar tendency, although less clearly, has been observed also for the transfer reactions for the $^8\text{He}+^{197}\text{Au}$ system at a similar energy.¹⁴⁰ This measurement also shows that the transfer cross sections for the ^8He projectile are considerably larger than those for the ^6He projectile at energies around the Coulomb barrier,¹⁴⁰ while these nuclei behave similar to each other in the subbarrier fusion reactions.¹⁴¹ Further theoretical studies are apparently necessary in order to understand the differences and the similarities of these Borromean nuclei, ^6He and ^8He , in several reaction processes at energies around the Coulomb barrier.

4. Heavier neutron-rich nuclei

4.1. Matter radii and neutron skin thickness

As we mentioned in Sec. 1, interaction cross sections σ_I are intimately related to the size of colliding nuclei.^{49,84} The interaction cross section is defined as a cross section for the change of the proton number Z and/or the neutron number N of a

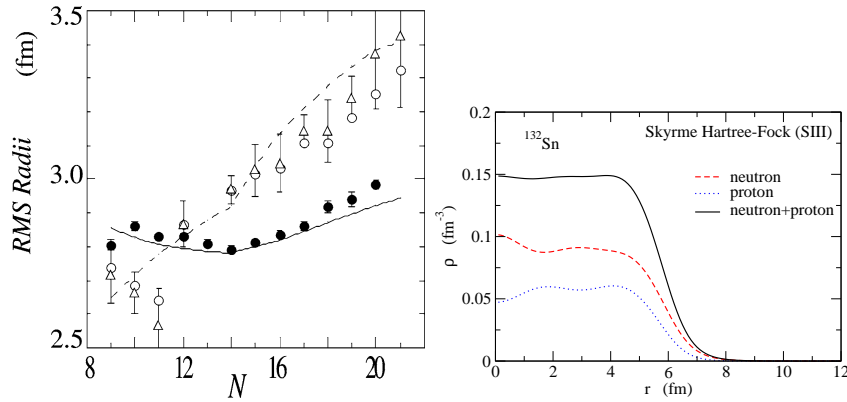


Fig. 17. The left panel: Neutron rms radii for Na isotopes (the open symbols). These are deduced from the measured interaction cross sections using the proton rms radii (the filled circles) obtained with the isotope shift measurements. Taken from Ref. 84. The right panel: the density distribution for ^{132}Sn obtained with the Skyrme-Hartree-Fock method with the SIII parameter set.

projectile nucleus after the interaction with a target nucleus. Another important quantity is a reaction cross section σ_R , which is defined as the total cross section minus elastic cross section, that is, the sum of the interaction cross section and the inelastic scattering cross section. Interaction cross sections are easier to measure than reaction cross sections, while the opposite is the case for a theoretical evaluation. For neutron-rich nuclei, cross sections for inelastic scattering are expected to be negligibly small at high incident energies,^{142–144} and the interaction cross sections are almost the same as the reaction cross sections. Because of this, measured interaction cross sections have often been compared to calculated reaction cross sections.

Reaction cross sections have often been analyzed by the Glauber theory.^{30,143,145,146} In the optical limit approximation to the Glauber theory, together with the zero range approximation to the nucleon-nucleon interaction, the reaction cross section is given by^{147,148}

$$\sigma_R = 2\pi \int_0^\infty b db \left[1 - \exp \left(-\sigma_{NN} \int d^2s \rho_P^{(z)}(\mathbf{s}) \rho_T^{(z)}(\mathbf{s} - \mathbf{b}) \right) \right], \quad (26)$$

where \mathbf{b} is the impact parameter and $\mathbf{s} = (x, y)$ is the plane perpendicular to z . σ_{NN} is the total NN cross section, and $\rho^{(z)}(\mathbf{s})$ is defined by $\rho^{(z)}(\mathbf{s}) = \int dz \rho(\mathbf{r})$, ρ_P and ρ_T being the projectile and the target densities, respectively. It has been known that the optical limit approximation overestimates reaction cross sections for weakly-bound nuclei.^{149–153} In order to cure this problem, Al-Khalili and Tostevin developed a few-body treatment for the Glauber theory.¹⁵² Abu-Ibrahim and Suzuki have also proposed another simple method which effectively takes into account the higher order corrections.¹⁵³

The left panel of Fig. 17 shows the neutron rms radii for Na isotopes (the open

symbols)⁸⁴ deduced from the measured interaction cross sections together with the proton rms radii (the filled circles) obtained from the isotope shift measurements. The figure indicates that the neutron rms radii are significantly larger than the proton rms radii for neutron-rich Na isotopes. This suggests that the neutron density distributions are largely extended over the proton density distributions, despite that there is no clear separation between a core nucleus and valence neutrons as in halo nuclei discussed in Sec. 2 and Sec. 3 (see Refs.154–159 for the halo structure in heavy nuclei). This structure is referred to as skin structure.^{160–162} It should be mentioned that the skin structure is not necessarily related to *s*- and *p*- wave single-particle orbits, in contrast to the halo structure.¹⁶¹ That is, the skin structure can be realized even with higher angular momentum states. As an example of skin nucleus, the right panel of Fig. 17 shows the density distribution for ¹³²Sn obtained with the Skyrme-Hartree-Fock method¹⁶³ with the SIII parameter set.¹⁶⁴

As we have discussed in Sec. 3.3, in order to discuss the skin thickness of neutron-rich nuclei, one needs both the matter and charge radii. For Na isotopes shown in Fig. 17, the proton radii have been obtained with the isotope shift measurements. The isotope shift measurement is not always applicable, however. In that case, one may use the charge changing cross section to estimate the rms radii for the proton distribution.^{165–169} This is the cross section for a change in the charge number *Z*, and is considered to be sensitive to the proton distribution.^{170,171} Alternatively, one may use the proton elastic scattering measurement.^{172,173} A yet novel method to extract the information on the proton distribution of neutron-rich nuclei is to use the electron scattering. Using a self-containing RI target (SCRIT), an attempt has already been successfully commenced at RIBF at RIKEN, Japan.^{174,175}

4.2. Odd-even staggering of interaction cross sections

The experimental interaction cross sections for neutron-rich nuclei often show a large odd-even staggering (OES). That is, the cross section for an odd-mass nucleus is significantly larger than the cross sections for the neighboring even-mass nuclei. A typical example is the interaction cross sections for ^{30,31,32}Ne, measured recently by Takechi *et al.* (see the left panel of Fig. 18).⁵⁰ In Ref. 176, the odd-even staggering was analyzed by introducing the staggering parameter defined as

$$\gamma_3 = (-)^A \frac{\sigma_I(A+1) - 2\sigma_I(A) + \sigma_I(A-1)}{2}, \quad (27)$$

where $\sigma_I(A)$ is the interaction cross section of a nucleus with mass number *A*. The right panel of Fig. 18 shows the experimental staggering parameter γ_3 for Ne isotopes as a function of the neutron separation energy for the odd-mass nuclei. It is compared with the results of the Hartree-Fock-Bogoliubov (HFB) calculations that takes into account the pairing correlations in the mean-field approximation. One can clearly see that the staggering parameter γ_3 increases rapidly for small

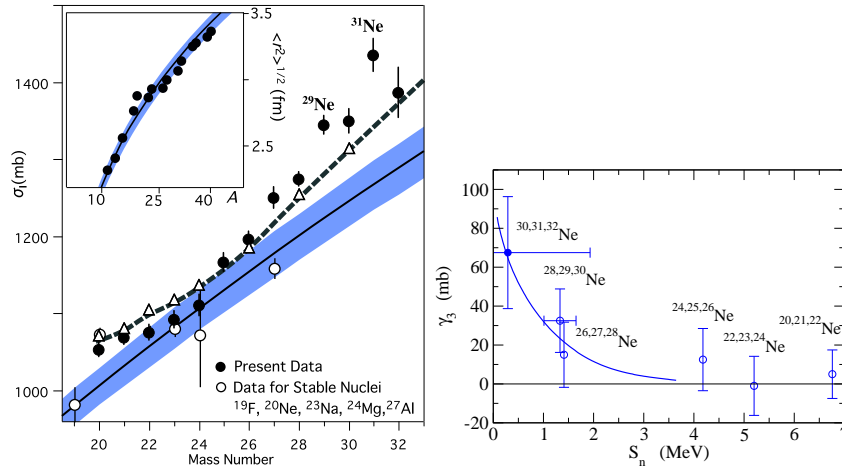


Fig. 18. The left panel: The experimental interaction cross sections for Ne isotopes with a carbon target at around 240 MeV/nucleon. The inset shows rms radii of stable nuclei. Taken from Ref. 50. The right panel: the odd-even staggering parameter defined by Eq. (27) for Ne isotopes as a function of the one-neutron separation energy for the odd-mass nuclei.¹⁷⁶ The solid line shows the result of the Hartree-Fock-Bogoliubov calculations.

separation energies, and goes up to a large value reaching $\gamma_3 \sim 80$ mb. Also, the experimental staggering parameters agree well with the HFB calculations, suggesting that the pairing correlation plays an important role in the odd-even staggering of the interaction cross sections.

4.3. Alpha cluster in neutron-rich nuclei

The α cluster model has been successful in describing the structure of light $N = Z$ nuclei.^{177,178} In neutron-rich nuclei, extra neutrons are surrounding tightly-bound alpha particles. A new theoretical framework, the antisymmetrized molecular dynamics (AMD), has been developed by Horiuchi *et al.*,¹⁷⁹ which has been successfully applied to neutron-rich nuclei.^{180–182} In this method, a many-body wave function is assumed to be a parity- and angular momentum projected Slater determinant with multi-centered Gaussian single-particle wave functions. Generator coordinate method (GCM) calculations with such Slater determinants have also been considered.¹⁸³ In this method, the alpha cluster is not assumed a priori, in contrast to the conventional cluster model, but it can emerge as a result of the energy minimization. The AMD calculations show that the cluster structure is developed and stabilized in some neutron-rich nuclei,¹⁸⁰ which can be well interpreted in terms of the molecular-orbital picture.^{184,185}

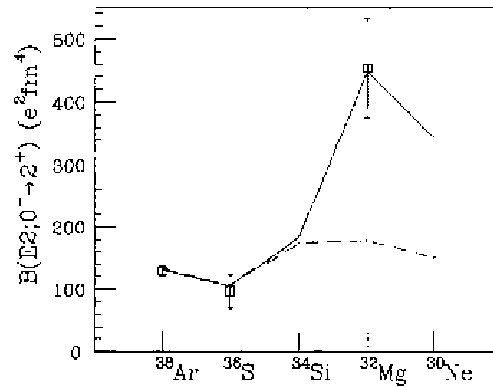


Fig. 19. The measured $B(E2)$ values for $N = 20$ even-even nuclei. The solid and the dashed lines are the results of the shell model calculation with the model space of sd+pf shells and sd shells, respectively. Taken from Ref. 196.

4.4. Shell evolution: change of spherical magic numbers in neutron-rich nuclei

The shell closures and the associated magic numbers are one of the most important concepts in nuclear physics.¹⁸⁶ For stable nuclei, these magic numbers correspond to 2, 8, 20, 28, 50, 82, and 126. That is, if either the neutron number or the proton number (or both) coincides with one of these numbers, that nucleus is particularly rigid and takes a spherical shape. In general, the first 2^+ state has a relatively large excitation energy in nuclei at the shell closures. However, a β -decay spectroscopy studies had revealed by the middle of 1980's that the first 2^+ state of the neutron-rich ^{32}Mg nucleus, which has $N = 20$, lies at as small as 0.886 MeV, suggesting a deformed shape of this nucleus.^{187–189} These experimental data stimulated lots of theoretical studies,^{190,191} in which the nuclei around ^{32}Mg have been referred to as the nuclei in the *island of inversion*.¹⁹¹ That is, the relative position between the deformed 2-particle-2-hole intruder state and the spherical 0-particle-0-hole state is inverted in this region. In 1995, Motobayashi *et al.* carried out the Coulomb excitation measurement of ^{32}Mg to the first 2^+ state, and extracted a large $B(E2)$ value.¹⁹² The large $B(E2)$ value is consistent with the nuclear deformation (see Fig. 19),^{193–195} and it has been concluded that the conventional $N = 20$ magic number does not hold in neutron-rich nuclei (see also Refs. 197 and 198). A similar disappearance of shell closure has been observed also for $N = 8$ ¹⁹⁹ and $N = 28$.²⁰⁰

A striking finding was that $N = 16$ becomes a spherical magic number in neutron-rich nuclei, accompanied by the disappearance of the $N = 20$ magicity. Ozawa *et al.* pointed out this fact by investigating systematically the neutron separation energy in the neutron-rich p - sd and the sd shell regions²⁰¹ (see also Refs. 202–205). When the neutron separation energy is plotted as a function of neutron number, it suddenly decreases across the shell closure. Ozawa *et al.* showed that it

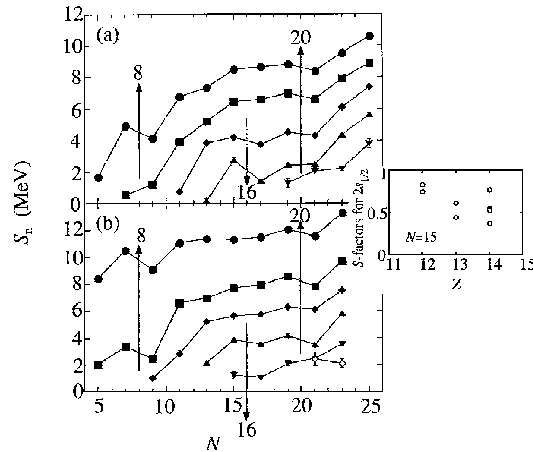


Fig. 20. Systematics of one neutron separation energy, S_n , for neutron-rich nuclei. The upper (a) and the lower (b) panels correspond to even- Z and odd- Z nuclei, respectively. The data for nuclei with same $N - Z$ are connected with the lines. For the upper (lower) panel, with decreasing order, the lines correspond to $N - Z = 1, 3, 5, 7$, and 9 ($N - Z = 0, 2, 4, 6$, and 8). A small panel on r.h.s. shows spectroscopic factors of $2s_{1/2}$ orbit in $N=15$ isotones. Taken from Ref. 201.

indeed happens at $N = 16$ for nuclei with $N - Z > 6$ (see Fig. 20),²⁰¹ indicating that the spherical magic number is shifted from $N = 20$ to 16 in neutron-rich nuclei. Notice that the new magic number $N = 16$ implies that the neutron-rich ^{24}O nucleus with $Z = 8$ and $N = 16$ is a double magic nucleus.^{206,207}

It is an important question to ask what makes the spherical magic numbers change in neutron-rich nuclei. Single-particle energies in a Woods-Saxon potential already show a quasi-degeneracy of $2s_{1/2}$ and $1d_{5/2}$ states and that the energy gap at $N = 16$ develops in weakly-bound systems.^{201,208} More microscopically, Otsuka *et al.* have argued that the tensor force as well as the spin-spin force of $(\sigma \cdot \sigma)(\tau \cdot \tau)$ type have a responsibility for the change of shell structure in neutron-rich nuclei.^{209,210} For instance, the attractive spin dependent interaction between the proton $d_{5/2}$ orbit and the neutron $d_{3/2}$ orbits leads to a down-shift of the neutron $d_{3/2}$ state in stable nuclei such as $^{30}_{14}\text{Si}_{16}$, making the conventional shell gap at $N = 20$. In the $^{24}_8\text{O}_{16}$ nucleus, on the other hand, the protons do not occupy the $d_{5/2}$ orbit, and thus this attraction does not work in the neutron orbits. Consequently, the energy shift of the neutron $d_{3/2}$ state does not happen, and the energy gap appears at $N = 16$.^{209,210} A similar effect may affect also the shell structure in heavier regions, *e.g.*, the magic numbers for superheavy elements.²¹¹

4.5. Deformed halo nuclei

In the vicinity of the stability line, it has been well known that many open-shell nuclei are deformed in the ground state. The nuclear deformation generates the collective rotational motion, which is characterized by a pronounced rotational spectrum

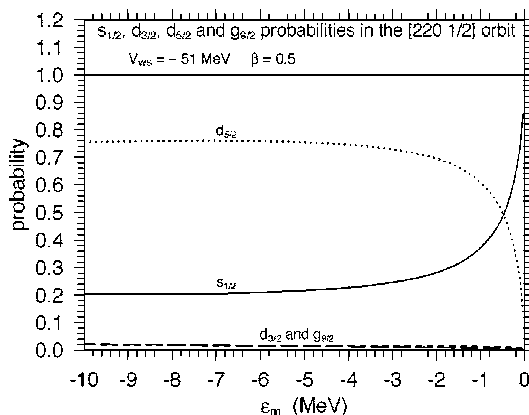


Fig. 21. The probability of each angular momentum component in a single-particle wave function in a deformed mean-field potential. It is plotted as a function of the corresponding single-particle energy, ϵ_m . Taken from Ref. 218.

as well as strongly enhanced quadrupole transition probabilities. As we mentioned in the previous subsection, the first evidence for nuclear deformation in neutron-rich nuclei was the observation of a low-lying state in the ^{32}Mg nucleus. Another well known example is the so called *parity inversion* phenomenon in ^{11}Be .²¹² If one used a naive spherical shell model, one would expect that the valence neutron in ^{11}Be occupies the $1p_{1/2}$ state in the ground state and the first excited states can be constructed by promoting the valence neutron to the sd shell, that is, the first excited state would be a positive parity state. However, the observed ground state of the ^{11}Be is $1/2^+$ state and the first excited state is $1/2^-$ state at 0.324 MeV.²¹³ This appears as if the $2s_{1/2}$ and the $1p_{1/2}$ states are inverted in energy. This parity inversion problem has been naturally explained by considering that ^{11}Be is a deformed nucleus.^{214–216}

A single-particle motion in a deformed mean-field potential is well known as a Nilsson orbit.^{2,3} As a deformed mean-field potential does not have rotational symmetry, the corresponding single-particle wave functions are obtained as a linear combination of several angular momentum components. Misu *et al.* have pointed out that the s -wave component, when it contributes, becomes dominant in a deformed wave function as the separation energy decreases, and eventually it gives a 100% contribution in the limit of zero separation (see Fig. 21).²¹⁷ They have also shown that the p -wave component becomes dominant for negative parity states, although it does not give a 100% contribution even in the zero binding limit.²¹⁷ See also Refs. 218 and 219 for related publications, and Refs.^{220,221} for self-consistent mean-field calculations for deformed halo nuclei.

As we discussed in Sec. 2.1, the halo structure has been attributed to an occupation of s or p single-particle orbit. The s and p wave dominance phenomenon in a deformed single-particle state suggests that the nuclear deformation enhances

a chance for a halo formation in weakly bound nuclei. The first evidence for a deformed halo was observed recently for the ^{31}Ne nucleus.^{50,52} For this nucleus, both the Coulomb breakup cross section and the interaction cross section are found to be large, which clearly suggest a halo structure of this nucleus. Although a naive shell model indicates an occupation of the $1f_{7/2}$ state by the valence neutron, the halo structure can be easily understood by considering a deformation, by which the p -wave component can be largely coupled in the wave function.^{222–224} For instance, Urata *et al.* have carried out a particle-rotor model calculation²¹⁴ for this nucleus and shown that $I^\pi = 3/2^-$ is a good candidate for the ground state of ^{31}Ne , in which the component of the $p_{3/2}$ state coupled to the ground state of ^{30}Ne is as large as 44.9%.²²³

4.6. Collective excitations of neutron-rich nuclei

It has been well known that there are variety of collective excitations in atomic nuclei.^{2,3,225,226} For stable nuclei, these collective motions are approximately classified either as isovector or isoscalar types, in which the proton and the neutron motions are out-of-phase or in-phase, respectively. In neutron-rich nuclei, on the other hand, the isovector and the isoscalar modes are coupled to each other due to a large asymmetry in proton and neutron numbers.^{227,228} That is, a collective state may have both the isoscalar and isovector characters. In the extreme case, a pure neutron mode, in which only neutrons contribute to the collective excitation, may arise in neutron-rich nuclei.^{229,230} A candidate for such neutron mode has been experimentally observed in ^{16}C .^{231–233}

There have also been lots of theoretical developments in descriptions of collective excitations in neutron-rich nuclei. Theoretically, the random phase approximation (RPA) has provided a convenient and useful method to describe excited states of many-fermion systems.²²⁵ In this method, excited phonon states are described as a superposition of many 1-particle 1-hole states. For weakly bound nuclei, the continuum effects play an essential role due to a much lower threshold energy compared to stable nuclei. The continuum RPA method was first developed by Shlomo and Bertsch,²³⁴ which was subsequently applied to self-consistent calculations of nuclear giant resonances with Skyrme interaction by Liu and Van Giai.²³⁵ Hamamoto, Sagawa, and Zhang have extensively applied this method to nuclear responses in neutron-rich nuclei.^{227,228,236,237} An extension of the continuum RPA to deformed nuclei has also been carried out by Nakatsukasa and Yabana.²³⁸ Another important development was to include the pairing effects in the continuum RPA. As we discussed in Sec. 3, the pairing and the continuum couplings play an essential role in neutron-rich nuclei. These effects can be taken into account by extending the RPA to the quasi-particle RPA (QRPA). The continuum QRPA method on top of the ground state described by the Hartree-Fock-Bogoliubov method has been developed by several groups,^{123,124,230,239–247} and has been applied to neutron-rich nuclei.

Recently, much attention has been paid to low-lying dipole (E1) strength in

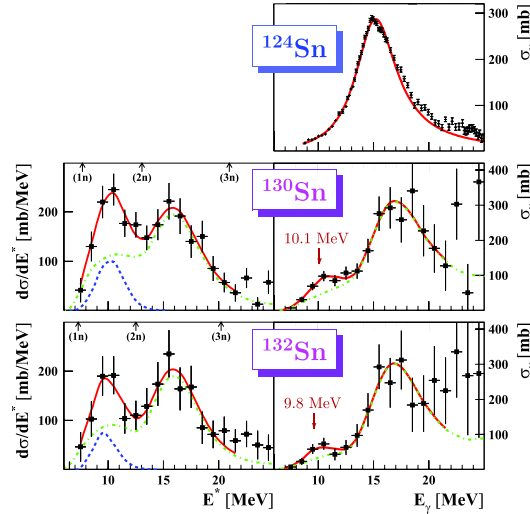


Fig. 22. The experimental data for the Coulomb excitation (the left panels) and the photo-neutron (the right panels) cross sections for ^{124}Sn , ^{130}Sn , and ^{132}Sn . Taken from Ref. 254.

neutron-rich nuclei, which has often been referred to as *pygmy dipole resonance*. It has been well known that the dipole strength is far dominated by the giant dipole response (GDR)^{225,226} (see also Ref. 248 for a recent complete measurement for the dipole strengths in ^{208}Pb over a wide range of excitation energy). However, nuclei with a neutron excess often show a low-lying dipole strength at energies much lower than the GDR. The pygmy dipole resonances have been experimentally found not only in neutron-rich nuclei^{249–255} but also in stable nuclei^{256–266} (see Fig. 22). The pygmy dipole resonance is important also from the astrophysical point of view, as it affects significantly a radiative neutron capture rate, which is relevant to the r-process nucleosynthesis.²⁶⁷ Although the exact nature of the pygmy dipole resonance has not yet been clarified completely, it has been pointed out that the pygmy dipole strength is strongly correlated with the neutron skin thickness^{268,269} (see, however, also a counter argument in Ref. 270). As the neutron skin thickness is intimately related to the equation of state (EOS) in asymmetric nuclear matter,²⁷¹ it is expected that the information on the nuclear matter properties, such as the symmetry energy coefficients, may be obtained by studying the pygmy dipole strength in neutron-rich nuclei.²⁵⁵

5. Summary

Physics of unstable nuclei has been developed rapidly thanks to the recent availability of radioactive beams in the world. A new era has been commenced in nuclear physics, where the isospin degree of freedom, that is one of the fundamental quantum numbers in atomic nuclei, can be controlled in self-bound interacting Fermion

systems. Many new features of atomic nuclei have been discovered or theoretically discussed so far, as we have reviewed in this Chapter. We list some of these below:

- (1) The most prominent discovery was the halo structure, in which the neutron density distribution largely extends over the proton distribution. In stable nuclei, the neutron and the proton distributions are similar to each other within a scaling factor, and thus the halo structure is a clear manifestation of the decoupling of proton and neutron in weakly bound nuclei. The halo structure is ascribed to an occupation of either s or p orbits, for which the root mean square radius diverges in the zero binding limit. Typical examples of the halo nuclei include ${}^6\text{He}$, ${}^{11}\text{Li}$, and ${}^{11}\text{Be}$. ${}^{31}\text{Ne}$ has also been identified recently as a deformed halo nucleus.
- (2) A similar decoupling effect is the skin structure. While the halo structure corresponds to a long low-density tail of neutron distribution, the skin structure corresponds to a layer of extremely neutron-rich matter. The matter radii of neutron-rich nuclei have been systematically studied with interaction cross section and isotope shift measurements.
- (3) Neutron-rich nuclei often show a soft dipole excitation, that is, dipole strengths in the low excitation energy region. For halo nuclei, the soft dipole mode is attributed to the threshold effect, that is, the optimal matching of wave functions between a weakly bound and continuum states. For skin nuclei, the low-lying dipole resonances have been referred to as the pygmy dipole mode. Even though the exact nature of the pygmy dipole mode has not yet been fully clarified, it has been expected that it is closely related to the equation of state of asymmetric nuclear matter.
- (4) The dineutron correlation in neutron-rich nuclei, such as ${}^{11}\text{Li}$ and ${}^6\text{He}$, has been theoretically predicted. This is a spatial correlation, with which two valence neutrons take a compact configuration. The recent experimental data for the Coulomb dissociation of ${}^{11}\text{Li}$ strongly suggests the existence of the dineutron correlation in ${}^{11}\text{Li}$. A similar correlation in proton rich nuclei, that is, the diproton correlation has also been predicted. The two-nucleon radioactivities as well as the two-neutron transfer reactions are expected to provide a direct probe of the dineutron correlation.
- (5) Another important feature in neutron-rich nuclei is the change of (spherical) magic numbers. It was considered that the magic numbers exist independently for proton and neutron. However in neutron-rich nuclei some of the magic numbers have been found to disappear ($N=8$ and 20) and a new spherical magic number appears ($N=16$). These changes have revealed the importance of tensor interaction.

A new generation RI beam facility, RIBF, at RIKEN, Japan, has already been in operation, and other new generation facilities, such as FAIR (Germany), SPIRAL2 (GANIL), and FRIB (USA), will also be in operation in a few years. We are now

at a stage in which we gain a deep insight in nuclear many-body systems, from stable nuclei to weakly-bound unstable nuclei in a unified manner, and are about to explore a vast *terra incognita*²⁷² in the nuclear chart.

Acknowledgments

We thank A. Vitturi, P. Schuck, H. Esbensen, G. Colo, J. Margueron, T. Oishi, Y. Urata, T. Nakamura, S. Shimoura, H. Sakurai, A. Navin, M. Takechi, and L. Corradi for collaborations and many useful discussions. This work was supported by the Japanese Ministry of Education, Culture, Sports, Science and Technology by Grant-in-Aid for Scientific Research under program no. (C) 22540262.

References

1. H.A. Bethe and R.F. Bacher, Rev. Mod. Phys. **8**, 82 (1936); H.A. Bethe, Rev. Mod. Phys. **9**, 69 (1937).
2. A. Bohr and B.R. Mottelson, *Nuclear Structure Vol. I* (Benjamin, Reading, MA, 1969); *Nuclear Structure Vol. II* (Benjamin, Reading, MA, 1975).
3. P. Ring and P. Schuck, *The Nuclear Many Body Problem* (Springer-Verlag, New York, 1980).
4. G.T. Garvey, Comments on Nucl. and Part. Phys. **5** (1972) 85.
5. O.L. Keller Jr., Comments on Nucl. and Part. Phys. **5** (1972) 98.
6. V.V. Volkov, in Proceedings of the International Conference on Nuclear Physics, ed. by J. de Boer and H.J. Mang (North Holland Pub. Co., Amsterdam, 1973), vol.2, p. 280.
7. *Proc. of International Symposium on Why and How Should We Investigate Nuclides Far Off the Stability Line*, ed. by W. Forsling, C.J. Herrlander, and H. Ryde (Almqvist and Wiksell, Stockholm, 1967).
8. *Proc. of International Conference on the Properties of Nuclei Far From the Region of Beta-Stability* (CERN Report No. 70-30, 1970).
9. G.T. Garvey and I. Kelson, Phys. Rev. Lett. **16** (1966) 197.
10. I. Tanihata, H. Hamagaki, O. Hashimoto, Y. Shida, N. Yoshikawa, K. Sugimoto, O. Yamakawa, T. Kobayashi, and N. Takahashi, Phys. Rev. Lett. **55** (1985) 2676.
11. A.H. Wapstra, G. Audi, and K. Bos, Nucl. Phys. **A432** (1985) 1.
12. C. Bachelet, G. Audi, C. Gaulard, C. Guenaut, F. Herfurth, D. Lunney, M. de Saint Simon, and C. Thibault, Phys. Rev. Lett. **100** (2008) 182501.
13. P.G. Hansen and B. Jonson, Europhys. Lett. **4** (1987) 409.
14. T. Kobayashi, O. Yamakawa, K. Omata, K. Sugimoto, T. Shimoda, N. Takahashi, and I. Tanihata, Phys. Rev. Lett. **60** (1988) 2599.
15. T. Motobayashi, Nucl. Phys. **A834** (2010) 707C; H. Sakurai, Nucl. Phys. **A834** (2010) 388C.
16. I. Augustin, Nucl. Inst. Methods Phys. Res. **B261** (2007) 1014.
17. S. Gales, Nucl. Phys. **A834** (2010) 717C.
18. M. Thoennessen, Nucl. Phys. **A834** (2010) 688C.
19. A.C. Mueller and B.M. Sherrill, Ann. Rev. Nucl. Phys. Sci. **43** (1993) 529.
20. I. Tanihata, Prog. Part. Nucl. Phys. **35** (1995) 505.
21. P.G. Hansen, A.S. Jensen, and B. Jonson, Ann. Rev. Nucl. Part. Sci. **45** (1995) 591.
22. I. Tanihata, J. of Phys. **G22** (1996) 157.

23. I. Tanihata, Nucl. Inst. Methods Phys. Res. **B266** (2008) 4067.
24. P.G. Hansen and J.A. Tostevin, Ann. Rev. Nucl. Part. Sci. **53** (2003) 219.
25. B. Jonson, Phys. Rep. **389** (2004) 1.
26. A.S. Jensen, K. Riisager, D.V. Fedorov, and E. Garrido, Rev. Mod. Phys. **76** (2004) 215.
27. K. Ikeda, T. Myo, K. Kato, and H. Toki, Lec. Notes in Phys. **818** (2010) 165.
28. T. Nakamura and Y. Kondo, Lec. Notes in Phys. **848** (2012) 67.
29. M. Pfützner, M. Karny, L.V. Grigorenko, and K. Riisager, Rev. Mod. Phys., in press. e-print: arXiv:1111.0482v1 [nucl-ex].
30. J. Al-Khalili and F. Nunes, J. of Phys. **G29** (2003) R89.
31. M. Yahiro, K. Ogata, T. Matsumoto, and K. Minomo, arXiv:11203.5392 [nucl-th].
32. L.F. Canto, P.R.S. Gomes, R. Donangelo, and M.S. Hussein, Phys. Rep. **424** (2006) 1.
33. N. Paar, D. Vretenar, E. Khan, and G. Colo, Rep. Prog. Phys. **70** (2007) 691.
34. I. Tanihata, T. Kobayashi, O. Yamakawa, S. Shimoura, K. Ekuni, K. Sugimoto, N. Takahashi, T. Shimoda, and H. Sato, Phys. Lett. **B206** (1988) 592.
35. G. Audi and A.H. Wapstra, Nucl. Phys. **A565** (1993) 66.
36. M. Fukuda, T. Ichihara, N. Inabe, T. Kubo, H. Kumagai, T. Nakagawa, Y. Yano, I. Tanihata, M. Adachi, K. Asahi, M. Kouguchi, M. Ishihara, H. Sagawa, and S. Shimoura, Phys. Lett. **B268** (1991) 339.
37. K. Riisager, A.S. Jensen and P. Møller, Nucl. Phys. **A548** (1992) 393.
38. H. Sagawa, Phys. Lett. **B286** (1992) 7.
39. K. Ikeda, INS Report JHP-7 (1988), in Japanese; Nucl. Phys. **A538** (1992) 355c.
40. J.M. Blatt and V.F. Weisskopf, *Theoretical Nuclear Physics*, (John Wiley & Sons, New York, 1952).
41. C.A. Bertulani, G. Baur, and M.S. Hussein, Nucl. Phys. **A526** (1991) 751.
42. H. Sagawa, N. Van Giai, N. Takigawa, M. Ishihara, and K. Yazaki, Z. Phys. **A351** (1995) 385.
43. T. Otsuka, M. Ishihara, N. Fukunishi, T. Nakamura, M. Yokoyama, Phys. Rev. **C49** (1994) R2289.
44. M.A. Nagarajan, S.M. Lenzi, and A. Vitturi, Euro. Phys. J. **A24** (2005) 63.
45. S. Typel and G. Baur, Nucl. Phys. **A759** (2005) 247.
46. C.A. Bertulani and G. Baur, Phys. Rep. **163**, 299 (1988); Nucl. Phys. **A480** (1988) 615.
47. A. Winther and K. Alder, Nucl. Phys. **A319** (1979) 518.
48. T. Nakamura, S. Shimoura, T. Kobayashi, T. Teranishi, K. Abe, N. Aoi, Y. Doki, M. Fujimaki, N. Inabe, N. Iwasa, K. Katori, T. Kubo, H. Okuno, T. Suzuki, I. Tanihata, Y. Watanabe, A. Yoshida, and M. Ishihara, Phys. Lett. **B331** (1994) 296.
49. A. Ozawa, O. Bochkarev, L. Chulkov, D. Cortina, H. Geissel, M. Hellström, M. Ivanov, R. Janik, K. Kimura, T. Kobayashi, A.A. Korshennikov, G. Münzenberg, F. Nickel, Y. Ogawa, A.A. Ogloblin, M. Pfützner, V. Pribora, H. Simon, B. Sitar, P. Strmen, K. Sümmerer, T. Suzuki, I. Tanihata, M. Winkler, K. Yoshida, Nucl. Phys. **A691** (2001) 599.
50. M. Takechi, T. Ohtsubo, M. Fukuda, D. Nishimura, T. Kuboki, T. Suzuki, T. Yamaguchi, A. Ozawa, T. Moriguchi, H. Ooishi, D. Nagae, H. Suzuki, S. Suzuki, T. Izumikawa, T. Sumikama, M. Ishihara, H. Geissel, N. Aoi, Rui-Jiu Chen, De-Qing Fang, N. Fukuda, I. Hachiuma, N. Inabe, Y. Ishibashi, Y. Ito, D. Kameda, T. Kubo, K. Kusaka, M. Lantz, Yu-Gang Ma, K. Matsuta, M. Mihara, Y. Miyashita, S. Momota, K. Namihira, M. Nagashima, Y. Ohkuma, T. Ohnishi, M. Ohtake, K. Ogawa, H. Sakurai, Y. Shimbara, T. Suda, H. Takeda, S. Takeuchi, K. Tanaka, R. Watanabe,

- M. Winkler, Y. Yanagisawa, Y. Yasuda, K. Yoshinaga, A. Yoshida, K. Yoshida, Phys. Lett. **B707** (2012) 357.
51. T. Nakamura, N. Fukuda, T. Kobayashi, N. Aoi, H. Iwasaki, T. Kubo, A. Mengoni, M. Notani, H. Otsu, H. Sakurai, S. Shimoura, T. Teranishi, Y.X. Watanabe, K. Yoneda, and M. Ishihara, Phys. Rev. Lett. **83** (1999) 1112.
 52. T. Nakamura, N. Kobayashi, Y. Kondo, Y. Satou, N. Aoi, H. Baba, S. Deguchi, N. Fukuda, J. Gibelin, N. Inabe, M. Ishihara, D. Kamada, Y. Kawada, T. Kubo, K. Kusaka, A. Mengoni, T. Motobayashi, T. Ohnishi, M. Ohtake, N.A. Orr, H. Otsu, T. Otsuka, A. Saito, H. Sakurai, S. Shimoura, T. Sumikama, H. Takeda, E. Takeshita, M. Takechi, S. Takeuchi, K. Tanaka, K.N. Tanaka, N. Tanaka, Y. Togano, Y. Utsuno, K. Yoneda, A. Yoshida, and K. Yoshida, Phys. Rev. Lett. **103** (2009) 262501.
 53. J. Dobaczewski, W. Nazarewicz, T.R. Werner, J.F. Berger, C.R. Chimm, and J. Decharge, Phys. Rev. C **53** (1996) 2809.
 54. M. Bender, P.-H. Heenen, and P.-G. Reinhard, Rev. Mod. Phys. **75** (2003) 121.
 55. D.M. Brink and R.A. Broglia, *Nuclear Superfluidity: Pairing in Finite Systems*, (Cambridge University Press, Cambridge, 2005).
 56. S.Y. Chang and G.F. Bertsch, Phys. Rev. A **76** (2007) 021603(R).
 57. M.G. Endres, D.B. Kaplan, J.-W. Lee, and A.N. Nicholson, Phys. Rev. A **84** (2011) 043644.
 58. G.F. Bertsch and H. Esbensen, Ann. Phys. (N.Y.) **209** (1991) 327.
 59. M.V. Zhukov, B.V. Danilin, D.V. Fedorov, J.M. Bang, I.J. Thompson, and J.S. Vaagen, Phys. Rep. **231** (1993) 151.
 60. G.F. Bertsch, R.A. Broglia, and C. Riedel, Nucl. Phys. A **91** (1967) 123.
 61. A.B. Migdal, Soviet J. of Nucl. Phys. **16** (1973) 238.
 62. F. Catara, A. Insolia, E. Maglione, and A. Vitturi, Phys. Rev. C **28** (1984) 1091.
 63. R.H. Ibarra, N. Austern, M. Vallieres, and D.H. Feng, Nucl. Phys. A **288** (1977) 397.
 64. N. Pillet, N. Sandulescu, and P. Schuck, Phys. Rev. C **76** (2007) 024310.
 65. K. Hagino, H. Sagawa, and P. Schuck, J. of Phys. G **37** (2010) 06404.
 66. F. Barranco, P.F. Bortignon, R.A. Broglia, G. Colo, and E. Vigezzi, Eur. Phys. J. A **11** (2001) 385.
 67. K. Hagino and H. Sagawa, Phys. Rev. C **72** (2005) 044321; Phys. Rev. C **76** (2007) 021301.
 68. K. Hagino, H. Sagawa, J. Carbonell, and P. Schuck, Phys. Rev. Lett. **99** (2007) 022506.
 69. Y. Kikuchi, K. Kato, T. Myo, M. Takashina, and K. Ikeda, Phys. Rev. C **81** (2010) 044308.
 70. K. Hagino, N. Takahashi, and H. Sagawa, Phys. Rev. C **77** (2008) 054317.
 71. N. Itagaki, M. Ito, K. Arai, S. Aoyama, and T. Kokalova, Phys. Rev. C **78** (2008) 017306.
 72. Y. Kanada-En'yo, Phys. Rev. C **76** (2007) 044323.
 73. M. Matsuo, K. Mizuyama, and Y. Serizawa, Phys. Rev. C **71** (2005) 064326.
 74. S. Aoyama and N. Itagaki, Phys. Rev. C **80** (2009) 021304.
 75. M. Matsuo, Phys. Rev. C **73** (2006) 044309.
 76. J. Margueron, H. Sagawa, and K. Hagino, Phys. Rev. C **76** (2007) 064316.
 77. Y. Kanada-En'yo, N. Hinohara, T. Suhara, and P. Schuck, Phys. Rev. C **79** (2009) 054305.
 78. T. Oishi, K. Hagino, and H. Sagawa, Phys. Rev. C **82** (2010) 024315.
 79. T. Nakamura, A.M. Vinodkumar, T. Sugimoto, N. Aoi, H. Baba, D. Bazin, N. Fukuda, T. Gomi, H. Hasegawa, N. Imai, M. Ishihara, T. Kobayashi, Y. Kondo, T. Kubo, M. Miura, T. Motobayashi, H. Otsu, A. Saito, H. Sakurai, S. Shimoura, K. Watanabe, Y.X. Watanabe, T. Yakushiji, Y. Yanagisawa, and K. Yoneda, Phys. Rev. Lett. **96**

- (2006) 252502.
80. T. Aumann, D. Aleksandrov, L. Axelsson, T. Baumann, M.J.G. Borge, L.V. Chulkov, J. Cub, W. Dostal, B. Eberlein, Th. W. Elze, H. Emling, H. Geissel, V.Z. Goldberg, M. Golovkov, A. Grünschloss, M. Hellström, K. Hencken, J. Holeczek, R. Holzmann, B. Jonson, A.A. Korshenninikov, J.V. Kratz, G. Kraus, R. Kulesa, Y. Leifels, A. Leistenschneider, T. Leth, I. Mukha, G. Münzenberg, F. Nickel, T. Nilsson, G. Nyman, B. Petersen, M. Pfützner, A. Richter, K. Riisager, C. Scheidenberger, G. Schrieder, W. Schwab, H. Simon, M. H. Smedberg, M. Steiner, J. Stroth, A. Surowiec, T. Suzuki, O. Tengblad, and M. V. Zhukov, *Phys. Rev. C* **59** (1999) 1252.
 81. H. Esbensen, K. Hagino, P. Mueller, and H. Sagawa, *Phys. Rev. C* **76** (2007) 024302.
 82. K. Hagino, H. Sagawa, T. Nakamura, and S. Shimoura, *Phys. Rev. C* **80** (2009) 047301.
 83. H. Esbensen and G.F. Bertsch, *Nucl. Phys. A* **542** (1992) 310.
 84. A. Ozawa, T. Suzuki, and I. Tanihata, *Nucl. Phys. A* **693** (2001) 32.
 85. Z.-C. Yan and G. W. F. Drake, *Phys. Rev. Lett.* **91** (2003) 113004.
 86. L.-B. Wang, P. Mueller, K. Bailey, G.W.F. Drake, J.P. Greene, D. Henderson, R.J. Holt, R.V.F. Janssens, C.L. Jiang, Z.-T. Lu, T.P. O'Connor, R.C. Pardo, K.E. Rehm, J.P. Schiffer, and X. D. Tang, *Phys. Rev. Lett.* **93** (2004) 142501.
 87. P. Mueller, I.A. Sulai, A.C.C. Villari, J.A. Alcantara-Nunez, R. Alves-Conde, K. Bailey, G.W.F. Drake, M. Dubois, C. Eleon, G. Gaubert, R.J. Holt, R.V.F. Janssens, N. Lecesne, Z.-T. Lu, T.P. O'Connor, M.-G. Saint-Laurent, J.-C. Thomas, and L.-B. Wang, *Phys. Rev. Lett.* **99** (2007) 252501.
 88. R. Sanchez, W. Nörtershäuser, G. Ewald, D. Albers, J. Behr, P. Bricault, B.A. Bushaw, A. Dax, J. Dilling, M. Dombisky, G.W.F. Drake, S. Götte, R. Kirchner, H.-J. Kluge, Th. Kuhl, J. Lassen, C.D.P. Levy, M.R. Pearson, E.J. Prime, V. Ryjkov, A. Wojtaszek, Z.-C. Yan, and C. Zimmermann, *Phys. Rev. Lett.* **96** (2006) 033002.
 89. W. Nörtershäuser, D. Tiedemann, M. Zakova, Z. Andjelkovic, K. Blaum, M.L. Bissell, R. Cazan, G.W.F. Drake, Ch. Geppert, M. Kowalska, J. Kramer, A. Krieger, R. Neugart, R. Sanchez, F. Schmidt-Kaler, Z.-C. Yan, D. T. Yordanov, and C. Zimmermann, *Phys. Rev. Lett.* **102** (2009) 062503.
 90. G. Ewald, W. Nörtershäuser, A. Dax, S. Götte, R. Kirchner, H.-J. Kluge, Th. Kuhl, R. Sanchez, A. Wojtaszek, B.A. Bushaw, G.W.F. Drake, Z.-C. Yan, and C. Zimmermann, *Phys. Rev. Lett.* **93** (2004) 113002.
 91. W. Nörtershäuser, R. Sanchez, G. Ewald, A. Dax, J. Behr, P. Bricault, B.A. Bushaw, J. Dilling, M. Dombisky, G.W.F. Drake, S. Götte, H.-J. Kluge, Th. Kuhl, J. Lassen, C. D. P. Levy, K. Pachucki, M. Pearson, M. Puchalski, A. Wojtaszek, Z.-C. Yan, C. Zimmermann, *Phys. Rev. A* **83** (2011) 012516.
 92. W. -M. Yao *et al.* (Particle Data Group), *J. Phys. G* **33** (2006) 1.
 93. J.L. Friar, J. Martorell, and D.W.L. Sprung, *Phys. Rev. A* **56** (1997) 4579.
 94. K. Varga, Y. Suzuki, and Y. Ohbayasi, *Phys. Rev. C* **50** (1994) 189.
 95. H. Esbensen, G.F. Bertsch, and K. Hencken, *Phys. Rev. C* **56** (1997) 3054.
 96. S. Funada, H. Kameyama, and Y. Sakuragi, *Nucl. Phys. A* **575** (1994) 93.
 97. E. Caurier and P. Navratil, *Phys. Rev. C* **73** (2006) 021302(R).
 98. Y. Kanada-En'yo, *Phys. Rev. C* **76** (2007) 044323.
 99. Y. Shen and Z. Ren, *Phys. Rev. C* **54** (1996) 1158.
 100. T. Myo, Y. Kikuchi, K. Kato, H. Toki, and K. Ikeda, *Prot. Theo. Phys.* **119** (2008) 561.
 101. I.Tanihata, D.Hirata, T.Kobayashi, S.Shimoura, K.Sugimoto, and H.Toki, *Phys. Lett. B* **289** (1992) 261.
 102. K. Hagino and H. Sagawa, *Phys. Rev. C* **76** (2007) 047302.
 103. C.A. Bertulani and M.S. Hussein, *Phys. Rev. C* **76** (2007) 051602.

104. P.J. Woods and C.N. Davids, *Ann. Rev. Nucl. Part. Sci.* **47** (1997) 541.
105. B. Blank and M. Ploszajczak, *Rep. Prog. Phys.* **71** (2008) 046301.
106. L.V. Grigorenko, *Phys. of Part. and Nucl.* **40** (2009) 674, and references therein.
107. L.V. Grigorenko, T.D. Wiser, K. Mercurio, R.J. Charity, R. Shane, L.G. Sobotka, J.M. Elson, A.H. Wuosmaa, A. Banu, M. McCleskey, L. Trache, R.E. Tribble, and M.V. Zhukov, *Phys. Rev.* **C80** (2009) 034602.
108. A.A. Sonzogni, C.N. Davids, P.J. Woods, D. Seweryniak, M.P. Carpenter, J.J. Ressler, J. Schwartz, J. Uusitalo, and W.B. Walters, *Phys. Rev. Lett.* **83** (1999) 1116.
109. M. Karny, R. Grzywacz, J.C. Batchelder, C.R. Bingham, C.J. Gross, K. Hagino, J.H. Hamilton, Z. Janas, W.D. Kulp, J.W. McConnell, M. Momayezi, A. Piechaczek, K. Rykaczewski, P.A. Semmes, J.A. Winger, and E.F. Zganjar, *Phys. Rev. Lett.* **90** (2003) 012502.
110. M.N. Tantawy, C.R. Bingham, K.P. Rykaczewski, J.C. Batchelder, W. Krolas, M. Danchev, D. Fong, T.N. Ginter, C.J. Gross, R. Grzywacz, K. Hagino, J.H. Hamilton, D.J. Hartley, M. Karny, K. Li, C. Mazzocchi, A. Piechaczek, A.V. Ramayya, K. Rykaczewski, D. Shapira, A. Stolz, J.A. Winger, C.-H. Yu, and E.F. Zganjar, *Phys. Rev.* **C73** (2006) 024316.
111. V.I. Goldansky, *Nucl. Phys.* **19** (1960) 482.
112. M. Pfützner, E. Badura, C. Bingham, B. Blank, M. Chartier, H. Geissel, J. Giovino, L.V. Grigorenko, R. Grzywacz, M. Hellström, Z. Janas, J. Kurcewicz, A.S. Lalleman, C. Mazzocchi, I. Mukha, G. Müntenberg, C. Plettner, E. Roeckl, K.P. Rykaczewski, K. Schmidt, R.S. Simon, M. Stanoiu, and J.-C. Thomas, *Eur. Phys. J.* **A14** (2002) 279.
113. J. Giovino, B. Blank, M. Chartier, S. Czajkowski, A. Fleury, M. J. Lopez Jimenez, M.S. Pravikoff, J.-C. Thomas, F. de Oliveira Santos, M. Lewitowicz, V. Maslov, M. Stanoiu, R. Grzywacz, M. Pfützner, C. Borcea, and B.A. Brown, *Phys. Rev. Lett.* **89** (2002) 102501.
114. K. Miernik, W. Dominik, Z. Janas, M. Pfützner, L. Grigorenko, C.R. Bingham, H. Czyrkowski, M. Cwiok, I.G. Darby, R. Dabrowski, T. Ginter, R. Grzywacz, M. Karny, A. Korgul, W. Kusmierz, S.N. Liddick, M. Rajabali, K. Rykaczewski, and A. Stolz, *Phys. Rev. Lett.* **99** (2007) 192501.
115. M. Pomorski, M. Pfützner, W. Dominik, R. Grzywacz, T. Baumann, J. S. Berryman, H. Czyrkowski, R. Dbrowski, T. Ginter, J. Johnson, G. Kaminski, A. Kuzniak, N. Larson, S.N. Liddick, M. Madurga, C. Mazzocchi, S. Mianowski, K. Miernik, D. Miller, S. Paulauskas, J. Pereira, K.P. Rykaczewski, A. Stolz, and S. Suchyta, *Phys. Rev.* **C83** (2011) 061303(R).
116. A. Spyrou, Z. Kohley, T. Baumann, D. Bazin, B.A. Brown, G. Christian, P. A. DeYoung, J.E. Finck, N. Frank, E. Lunderberg, S. Mosby, W.A. Peters, A. Schiller, J.K. Smith, J. Snyder, M.J. Strongman, M. Thoennessen, and A. Volya, *Phys. Rev. Lett.* **108** (2012) 102501.
117. S. Yoshida, *Nucl. Phys.* **33** (1962) 685.
118. W. von Oertzen and A. Vitturi, *Rep. Prog. Phys.* **64** (2001) 1247, and references therein.
119. E. Plumbi, M. Grasso, D. Beaumel, E. Khan, J. Margueron, and J. van de Wiele, *Phys. Rev.* **C83** (2011) 034613.
120. M. Grasso, D. Lacroix, and A. Vitturi, *Phys. Rev.* **C85** (2012) 034317.
121. W. von Oertzen, H.G. Bohlen, B. Gebauer, R. Künkel, F. Pühlhofer and D. Scühhll, *Z. Phys.* **A326** (1987) 463.
122. L. Corradi, S. Szilner, G. Pollarolo, G. Coloo, P. Mason, E. Farnea, E. Fioretto, A. Gadea, F. Haas, D. Jelavic-Malenica, N. Marginean, C. Michelagnoli, G. Montagnoli,

- D. Montanari, F. Scarlassara, N. Soic, A.M. Stefanini, C.A. Ur, and J.J. Valiente-Dobon, *Phys. Rev.* **C84** (2011) 034603.
123. E. Khan, N. Sandulescu, N. Van Giai, and M. Grasso, *Phys. Rev.* **C69** (2004) 014314.
 124. H. Shimoyama and M. Matsuo, *Phys. Rev.* **C84** (2011) 044317.
 125. A. Insolia, R.J. Liotta, and E. Maglione, *J. of Phys.* **G15** (1989) 1249.
 126. G. Potel, F. Barranco, F. Marini, A. Idini, E. Vigezzi, and R.A. Broglia, *Phys. Rev. Lett.* **107** (2011) 092501.
 127. B.F. Bayman and J. Chen, *Phys. Rev.* **C26** (1982) 1509.
 128. M.A. Franey, B.F. Bayman, J.S. Lilley, and W.R. Phillips, *Phys. Rev. Lett.* **41** (1978) 837.
 129. H. Esbensen, C.L. Jiang, and K.E. Rehm, *Phys. Rev.* **C57** (1998) 2401.
 130. D.M. Brink, *Phys. Lett.* **B40** (1972) 37.
 131. A. Vitturi and H.M. Sofia, to appear in *Prog. Theo. Phys. Suppl.*
 132. I. Tanihata, M. Alcorta, D. Bandyopadhyay, R. Bieri, L. Buchmann, B. Davids, N. Galinski, D. Howell, W. Mills, S. Mythili, R. Openshaw, E. Padilla-Rodal, G. Ruprecht, G. Sheffer, A. C. Shotter, M. Trinczek, P. Walden, H. Savajols, T. Roger, M. Caamano, W. Mittig, P. Roussel-Chomaz, R. Kanungo, A. Gallant, M. Notani, G. Savard, I.J. Thompson, *Phys. Rev. Lett.* **100** (2008) 192502.
 133. Y.T. Oganessian, V.I. Zagrebaev and J.S. Vaagen, *Phys. Rev. Lett.* **82** (1999) 4996.
 134. Y.T. Oganessian, V.I. Zagrebaev and J.S. Vaagen, *Phys. Rev.* **C60** (1999) 044605.
 135. R. Raabe, A. Piechaczek, A. Andreyev, D. Baye, W. Bradfield-Smith, S. Cherubini, T. Davinson, P. Descouvemont, A. Di Pietro, W. Galster, M. Huyse, A.M. Laird, J. McKenzie, W.F. Mueller, A. Ostrowski, A. Shotter, P. Van Duppen, and A. Wohr, *Phys. Lett.* **B458** (1999) 1.
 136. L. Giot, P. Roussel-Chomaz, C.E. Demonchy, W. Mittig, H. Savajols, N. Alamanos, F. Auger, A. Gillibert, C. Jouanne, V. Lapoux, L. Nalpas, E.C. Pollacco, J.L. Sida, F. Skaza, M.D. Cortina-Gil, J. Fernandez-Vasquez, R.S. Mackintosh, A. Pakou, S. Pita, A. Rodin, S. Stepantsov, G.M. Ter Akopian, K. Rusek, I.J. Thompson, and R. Wolski, *Phys. Rev.* **C71** (2005) 064311.
 137. A. Chatterjee, A. Navin, A. Shrivastava, S. Bhattacharyya, M. Rejmund, N. Keeley, V. Nanal, J. Nyberg, R. G. Pillay, K. Ramachandran, I. Stefan, D. Bazin, D. Beaumel, Y. Blumenfeld, G. de France, D. Gupta, M. Labiche, A. Lemasson, R. Lemmon, R. Raabe, J. A. Scarpaci, C. Simenel, and C. Timis, *Phys. Rev. Lett.* **101** (2008) 032701.
 138. G. Potel, F. Barranco, E. Vigezzi, and R.A. Broglia, *Phys. Rev. Lett.* **105** (2010) 172502.
 139. D.T. Khoa and W. von Oertzen, *Phys. Lett.* **B595** (2004) 193.
 140. A. Lemasson, A. Navin, M. Rejmund, N. Keeley, V. Zelevinsky, S. Bhattacharyya, A. Shrivastava, D. Bazin, D. Beaumel, Y. Blumenfeld, A. Chatterjee, D. Gupta, G. de France, B. Jacquot, M. Labiche, R. Lemmon, V. Nanal, J. Nyberg, R.G. Pillay, R. Raabe, K. Ramachandran, J.A. Scarpaci, C. Schmitt, C. Simenel, I. Stefan, and C.N. Timis, *Phys. Lett.* **B697** (2011) 454.
 141. A. Lemasson, A. Shrivastava, A. Navin, M. Rejmund, N. Keeley, V. Zelevinsky, S. Bhattacharyya, A. Chatterjee, G. de France, B. Jacquot, V. Nanal, R. G. Pillay, R. Raabe, and C. Schmitt, *Phys. Rev. Lett.* **103** (2009) 232701.
 142. A. Ozawa, T. Baumann, L. Chulkov, D. Cortina, U. Datta, J. Fernandez, H. Geissel, F. Hammache, K. Itahashi, M. Ivanov, R. Janik, T. Kato, K. Kimura, T. Kobayashi, K. Markenroth, M. Meister, G. Muenzenberg, T. Ohtsubo, S. Ohya, T. Okuda, A.A. Ogloblin, V. Pribora, M. Sekiguchi, B. Sitar, P. Strmen, S. Sugimoto, K. Sümmerer, T. Suzuki, I. Tanihata, and Y. Yamaguchi, *Nucl. Phys.* **A709** (2002) 60.
 143. Y. Ogawa, K. Yabana, and Y. Suzuki, *Nucl. Phys.* **A543** (1992) 722.

144. A. Kohama, K. Iida, and K. Oyamatsu, *Phys. Rev.* **C78** (2008) 061601(R).
145. R.J. Glauber, in *Lectures on Theoretical Physics*, edited by W.E. Brittin and L.C. Dunham (Interscience, New York, 1959), Vol. 1, p. 315.
146. Y. Ogawa, T. Kido, K. Yabana, and Y. Suzuki, *Prog. Theo. Phys. Suppl.* **142** (2001) 157.
147. P. Karol, *Phys. Rev.* **C11** (1975) 1203.
148. G.F. Bertsch, B.A. Brown, and H. Sagawa, *Phys. Rev.* **C39** (1989) 1154.
149. G.F. Bertsch, H. Esbensen, and A. Sustich, *Phys. Rev.* **C42** (1990) 758.
150. N. Takigawa, M. Ueda, M. Kuratani, and H. Sagawa, *Phys. Lett.* **B288** (1992) 244.
151. J.S. Al-Khalili and J.A. Tostevin, *Phys. Rev. Lett.* **76** (1996) 3903.
152. J.S. Al-Khalili, J.A. Tostevin, and I.J. Thompson, *Phys. Rev.* **C54** (1996) 1843; J.A. Tostevin and J.S. Al-Khalili, *Phys. Rev.* **C59** (1999) R5.
153. B. Abu-Ibrahim and Y. Suzuki, *Phys. Rev.* **C61** (2000) 051601(R); **C62** (2000) 034608.
154. V. Rotival and T. Duguet, *Phys. Rev.* **C79** (2009) 054308.
155. V. Rotival, K. Bennaceur, and T. Duguet, *Phys. Rev.* **C79** (2009) 054309.
156. J. Meng and P. Ring, *Phys. Rev. Lett.* **80** (1998) 460.
157. J. Meng, H. Toki, J.Y. Zeng, S.Q. Zhang, and S.-G. Zhou, *Phys. Rev.* **C65** (2002) 041302(R).
158. J. Terasaki, S.Q. Zhang, S.G. Zhou, and J. Meng, *Phys. Rev.* **C74** (2006) 054318.
159. M. Grasso, S. Yoshida, N. Sandulescu, and Nguyen Van Giai, *Phys. Rev.* **C74** (2006) 064317.
160. W.D. Myers and W.J. Swiatecki, *Nucl. Phys.* **A336** (1980) 267.
161. N. Fukunishi, T. Otsuka, and I. Tanihata, *Phys. Rev.* **C48** (1993) 1648.
162. S. Mizutori, J. Dobaczewski, G.A. Lalasissis, W. Nazarewicz, and P.-G. Reinhard, *Phys. Rev.* **C61** (2000) 044326.
163. D. Vautherin and D.M. Brink, *Phys. Rev.* **C5** (1972) 626.
164. M. Beiner, H. Flocard, Nguyen Van Giai, and P. Quentin, *Nucl. Phys.* **A238** (1975) 29.
165. B. Blank, J.-J. Gaimard, H. Geissel, K.-H. Schmidt, H. Stelzer, K. Sümmerer, D. Bazin, R. Del Moral, J.P. Dufour, A. Flueury, F. Hubert, H.-G. Clerc, and M. Steiner, *Z. Phys.* **A343** (1992) 375.
166. L.V. Chulkov, O.V. Bochkarev, D. Cortina-Gil, H. Geissel, M. Hellström, M. Ivanov, R. Janik, K. Kimura, T. Kobayashi, A.A. Korshennikov, G. Münzenberg, F. Nickel, A.A. Ogloblin, A. Ozawa, M. Pfützner, V.N. Pribora, M.V. Rozhkov, H. Simon, B. Sitar, P. Strmen, K. Sümmerer, T. Suzuki, I. Tanihata, M. Winkler, and K. Yoshida, *Nucl. Phys.* **A674** (2000) 330.
167. O.V. Bochkarev, L.V. Chulkov, P. Egelhof, H. Geissel, M.S. Golovkov, H. Irnich, Z. Janas, H. Keller, T. Kobayashi, G. Kraus, G. Münzenberg, F. Nickel, A.A. Ogloblin, A. Ozawa, A. Piechaczek, E. Roeckl, W. Schwab, K. Sümmerer, T. Suzuki, I. Tanihata, and K. Yoshida, *Eur. Phys. J.* **A1** (1998) 15.
168. T. Yamaguchi, M. Fukuda, S. Fukuda, G.W. Fan, I. Hachiuma, M. Kanazawa, A. Kitagawa, T. Kuboki, M. Lantz, M. Mihara, M. Nagashima, K. Namihira, D. Nishimura, Y. Okuma, T. Ohtsubo, S. Sato, T. Suzuki, M. Takechi, and W. Xu, *Phys. Rev.* **C82** (2010) 014609.
169. T. Yamaguchi, I. Hachiuma, A. Kitagawa, K. Namihira, S. Sato, T. Suzuki, I. Tanihata, and M. Fukuda, *Phys. Rev. Lett.* **107** (2011) 032502.
170. J. Meng, S.-G. Zhou, and I. Tanihata, *Phys. Lett.* **B532** (2002) 209.
171. A. Bhagwat and Y.K. Gambhir, *Phys. Rev.* **C69** (2004) 014315.
172. S. Terashima, H. Sakaguchi, H. Takeda, T. Ishikawa, M. Itoh, T. Kawabata, T.

- Murakami, M. Uchida, Y. Yasuda, M. Yosoi, J. Zenihiro, H.P. Yoshida, T. Noro, T. Ishida, S. Asaji, and T. Yonemura, *Phys. Rev. C* **77** (2008) 024317.
173. J. Zenihiro, H. Sakaguchi, T. Murakami, M. Yosoi, Y. Yasuda, S. Terashima, Y. Iwao, H. Takeda, M. Itoh, H. P. Yoshida, and M. Uchida, *Phys. Rev. C* **82** (2010) 044611.
174. M. Wakasugi, T. Emoto, Y. Furukawa, K. Ishii, S. Ito, T. Koseki, K. Kurita, A. Kuwajima, T. Masuda, A. Morikawa, M. Nakamura, A. Noda, T. Ohnishi, T. Shirai, T. Suda, H. Takeda, T. Tamae, H. Tongu, S. Wang, and Y. Yano, *Phys. Rev. Lett.* **100** (2008) 164801.
175. T. Suda, M. Wakasugi, T. Emoto, K. Ishii, S. Ito, K. Kurita, A. Kuwajima, A. Noda, T. Shirai, T. Tamae, H. Tongu, S. Wang, and Y. Yano, *Phys. Rev. Lett.* **102** (2009) 102501.
176. K. Hagino and H. Sagawa, *Phys. Rev. C* **85** (2012) 014303; *Phys. Rev. C* **85** (2012) 037604.
177. *Alpha-like Four-body Correlations and Molecular Aspects in Nuclei*, *Prog. Theo. Phys. Suppl.* **52** (1972).
178. *Comprehensive Study of Structure of Light Nuclei*, *Prog. Theo. Phys. Suppl.* **68** (1980).
179. A. Ono, H. Horiuchi, T. Maruyama, and A. Ohnishi, *Prog. Theo. Phys.* **87** (1992) 1185.
180. Y. Kanada-En'yo and H. Horiuchi, *Prog. Theo. Phys. Suppl.* **142** (2001) 205, and references therein.
181. Y. Kanada-En'yo and M. Kimura, *Lec. Notes in Phys.* **818** (2010) 129.
182. Y. Kanada-En'yo, M. Kimura, and A. Ono, arXiv:1202.1864v1 [nucl-th].
183. M. Kimura and H. Horiuchi, *Prog. Theo. Phys.* **111** (2004) 841; M. Kimura, *Phys. Rev. C* **69** (2004) 044319.
184. N. Itagaki, S. Okabe, and K. Ikeda, *Prog. Theo. Phys. Suppl.* **142** (2001) 297, and references therein.
185. N. Itagaki, T. Otsuka, K. Ikeda, and S. Okabe, *Phys. Rev. Lett.* **92** (2004) 142501.
186. M.G. Mayer, *Phys. Rev.* **75** (1949) 1969; O. Haxel, J.H.D. Jensen, and H.E. Suess, *Phys. Rev.* **75** (1949) 1766.
187. C. Detraz, D. Guillemaud, G. Huber, R. Klapisch, M. Langevin, F. Naulin, C. Thibault, L.C. Carraz, and F. Touchard, *Phys. Rev. C* **19** (1979) 164.
188. D. Guillemaud-Mueller, C. Detraz, M. Langevin, F. Naulin, M. De Saint-Simon, C. Thibault, F. Touchard, and M. Epherre, *Nucl. Phys.* **A426** (1984) 37.
189. B.H. Wildenthal and W. Chung, *Phys. Rev. C* **22** (1980) 2260.
190. X. Campi, H. Flocard, A.K. Kerman, and S. Koonin, *Nucl. Phys.* **A251** (1975) 193.
191. E.K. Warburton, J.A. Becker, and B.A. Brown, *Phys. Rev. C* **41** (1990) 1147.
192. T. Motobayashi, Y. Ikeda, K. Ieki, M. Inoue, N. Iwasa, T. Kikuchi, M. Kurokawa, S. Moriya, S. Ogawa, H. Murakami, S. Shimoura, Y. Yanagisawa, T. Nakamura, Y. Watanabe, M. Ishihara, T. Teranishi, H. Okuno, R.F. Casten, *Phys. Lett. B* **346** (1995) 9.
193. N. Fukunishi, T. Otsuka, and T. Sebe, *Phys. Lett. B* **296** (1992) 279.
194. Y. Utsuno, T. Otsuka, T. Mizusaki, and M. Honma, *Phys. Rev. C* **60** (1999) 054315.
195. Y. Utsuno, T. Otsuka, T. Glasmacher, T. Mizusaki, and M. Honma, *Phys. Rev. C* **70** (1999) 044307.
196. T. Otsuka and N. Fukunishi, *Phys. Rep.* **264** (1996) 297.
197. Zs. Dombradi, Z. Elekes, A. Saito, N. Aoi, H. Baba, K. Demichi, Zs. Fülöp, J. Gibelin, T. Gomi, H. Hasegawa, N. Imai, M. Ishihara, H. Iwasaki, S. Kanno, S. Kawai, T. Kishida, T. Kubo, K. Kurita, Y. Matsuyama, S. Michimasa, T. Minemura, T. Motobayashi, M. Notani, T. Ohnishi, H.J. Ong, S. Ota, A. Ozawa, H.K. Sakai, H.

- Sakurai, S. Shimoura, E. Takeshita, S. Takeuchi, M. Tamaki, Y. Togano, K. Yamada, Y. Yanagisawa, and K. Yoneda, *Phys. Rev. Lett.* **96** (2006) 182501.
198. P. Doornenbal, H. Scheit, N. Aoi, S. Takeuchi, K. Li, E. Takeshita, H. Wang, H. Baba, S. Deguchi, N. Fukuda, H. Geissel, R. Gernhäuser, J. Gibelin, I. Hachiuma, Y. Hara, C. Hinke, N. Inabe, K. Itahashi, S. Itoh, D. Kameda, S. Kanno, Y. Kawada, N. Kobayashi, Y. Kondo, R. Krücken, T. Kubo, T. Kuboki, K. Kusaka, M. Lantz, S. Michimasa, T. Motobayashi, T. Nakamura, T. Nakao, K. Namihira, S. Nishimura, T. Ohnishi, M. Ohtake, N.A. Orr, H. Otsu, K. Ozeki, Y. Satou, S. Shimoura, T. Sumikama, M. Takechi, H. Takeda, K.N. Tanaka, K. Tanaka, Y. Togano, M. Winkler, Y. Yanagisawa, K. Yoneda, A. Yoshida, K. Yoshida, and H. Sakurai, *Phys. Rev. Lett.* **103** (2009) 032501.
199. H. Iwasaki, T. Motobayashi, H. Akiyoshi, Y. Ando, N. Fukuda, H. Fujiwara, Zs. Fülöp, K.I. Hahn, Y. Higurashi, M. Hirai, I. Hisanaga, N. Iwasa, T. Kijima, T. Mine-mura, T. Nakamura, M. Notani, S. Ozawa, H. Sakurai, S. Shimoura, S. Takeuchi, T. Teranishi, Y. Yanagisawa, and M. Ishihara, *Phys. Lett.* **B481** (2000) 7.
200. B. Bastin, S. Grevy, D. Sohler, O. Sorlin, Zs. Dombradi, N.L. Achouri, J.C. Angeli-que, F. Azaiez, D. Baiborodin, R. Borcea, C. Bourgeois, A. Buta, A. Bürger, R. Chapman, J.C. Dalouzy, Z. Dlouhy, A. Drouard, Z. Elekes, S. Franchoo, S. Iacob, B. Laurent, M. Lazar, X. Liang, E. Lienard, J. Mrazek, L. Nalpas, F. Negoita, N.A. Orr, Y. Penionzhkevich, Zs. Podolyak, F. Pougheon, P. Rousset-Chomaz, M.G. Saint-Laurent, M. Stanoiu, and I. Stefan, *Phys. Rev. Lett.* **99** (2007) 022503.
201. A. Ozawa, T. Kobayashi, T. Suzuki, K. Yoshida, and I. Tanihata, *Phys. Rev. Lett.* **84** (2000) 5493.
202. R. Kanungo, I. Tanihata, and A. Ozawa, *Phys. Lett.* **B528** (2002) 58.
203. M.W. Cooper, S.L. Tabor, T. Baldwin, D.B. Campbell, C. Chandler, C.R. Hoffman, K.W. Kemper, J. Pavan, A. Pipidis, M.A. Riley, and M. Wiedeking, *Phys. Rev.* **C65** (2002) 051302(R).
204. J. Gibelin, D. Beaumel, T. Motobayashi, N. Aoi, H. Baba, Y. Blumenfeld, Zs. Dombradi, Z. Elekes, S. Fortier, N. Frascaria, N. Fukuda, T. Gomi, K. Ishikawa, Y. Kondo, T. Kubo, V. Lima, T. Nakamura, A. Saito, Y. Satou, E. Takeshita, S. Takeuchi, T. Teranishi, Y. Togano, A.M. Vinodkumar, Y. Yanagisawa, and K. Yoshida, *Phys. Rev.* **C75** (2007) 057306.
205. C.R. Hoffman, T. Baumann, D. Bazin, J. Brown, G. Christian, P.A. DeYoung, J.E. Finck, N. Frank, J. Hinnefeld, R. Howes, P. Mears, E. Mosby, S. Mosby, J. Reith, B. Rizzo, W. F. Rogers, G. Peaslee, W.A. Peters, A. Schiller, M.J. Scott, S.L. Tabor, M. Thoennessen, P.J. Voss, and T. Williams, *Phys. Rev. Lett.* **100** (2008) 152502.
206. C.R. Hoffman, T. Baumann, D. Bazin, J. Brown, G. Christian, D.H. Denby, P.A. DeYoung, J.E. Finck, N. Frank, J. Hinnefeld, S. Mosby, W.A. Peters, W.F. Rogers, A. Schiller, A. Spyrou, M.J. Scott, S.L. Tabor, M. Thoennessen, and P. Voss, *Phys. Lett.* **B672** (2009) 17.
207. R. Kanungo, C. Nociforo, A. Prochazka, T. Aumann, D. Boutin, D. Cortina-Gil, B. Davids, M. Diakaki, F. Farinon, H. Geissel, R. Gernhäuser, J. Gerl, R. Janik, B. Jonson, B. Kindler, R. Knobel, R. Krücken, M. Lantz, H. Lenske, Y. Litvinov, B. Lommel, K. Mahata, P. Maierbeck, A. Musumarra, T. Nilsson, T. Otsuka, C. Perro, C. Scheidenberger, B. Sitar, P. Strmen, B. Sun, I. Szarka, I. Tanihata, Y. Utsuno, H. Weick, M. Winkler, *Phys. Rev. Lett.* **102** (2009) 152501.
208. I. Hamamoto, S.V. Lukyanov, and X.Z. Zhang, *Nucl. Phys.* **A683** (2001) 255; I. Hamamoto, *J. Phys.* **G37** (2010) 055102.
209. T. Otsuka, T. Suzuki, R. Fujimoto, H. Grawe, and Y. Akaishi, *Phys. Rev. Lett.* **95** (2005) 232502.

210. T. Otsuka, R. Fujimoto, Y. Utsuno, B.A. Brown, M. Honma, and T. Mizusaki, Phys. Rev. Lett. **87** (2001) 082502.
211. T. Otsuka, T. Suzuki, and Y. Utsuno, Nucl. Phys. **A805** (2008) 127c.
212. I. Talmi and I. Unna, Phys. Rev. Lett. **4** (1960) 469.
213. F. Ajzenberg-Selove and C.L. Busch, Nucl. Phys. **A336** (1980) 1.
214. H. Esbensen, B.A. Brown, and H. Sagawa, Phys. Rev. **C51** (1995) 1274.
215. F.M. Nunes, I.J. Thompson, and R.C. Johnson, Nucl. Phys. **A596** (1996) 171.
216. I. Hamamoto and S. Shimoura, J. of Phys. **G34** (2007) 2715.
217. T. Misu, W. Nazarewicz, and S. Aberg, Nucl. Phys. **A614** (1997) 44.
218. I. Hamamoto, Phys. Rev. **C69** (2004) 041306(R).
219. K. Yoshida and K. Hagino, Phys. Rev. **C72** (2005) 064311.
220. S.-G. Zhou, J. Meng, P. Ring, and E.-G. Zhao, Phys. Rev. **C82** (2010) 011301(R).
221. L. Li, J. Meng, P. Ring, E.-G. Zhao, and S.-G. Zhou, Phys. Rev. **C85** (2012) 024312.
222. I. Hamamoto, Phys. Rev. **C81** (2010) 021304(R).
223. Y. Urata, K. Hagino, and H. Sagawa, Phys. Rev. **C83** (2011) 041303(R).
224. K. Minomo, T. Sumi, M. Kimura, K. Ogata, Y.R. Shimizu, and M. Yahiro, Phys. Rev. **C84** (2011) 034602; Phys. Rev. Lett. **108** (2012) 052503.
225. G.F. Bertsch and R.A. Broglia, *Oscillations in Finite Quantum Systems* (Cambridge University Press, Cambridge, 1994).
226. M.N. Harakeh and A. van der Woude, *Giant Resonances*, (Oxford University Press, Oxford, 2001).
227. I. Hamamoto, H. Sagawa, and X.Z. Zhang, Phys. Rev. **C55** (1997) 2361.
228. H. Sagawa, Prog. Theo. Phys. Suppl. **142** (2001) 1.
229. M. Yokoyama, T. Otsuka, and N. Fukunishi, Phys. Rev. **C52** (1995) 1122.
230. M. Matsuo, Nucl. Phys. **A696** (2001) 371.
231. H.J. Ong, N. Imai, D. Suzuki, H. Iwasaki, H. Sakurai, T.K. Onishi, M.K. Suzuki, S. Ota, S. Takeuchi, T. Nakao, Y. Togano, Y. Kondo, N. Aoi, H. Baba, S. Bishop, Y. Ichikawa, M. Ishihara, T. Kubo, K. Kurita, T. Motobayashi, T. Nakamura, T. Okumura, and Y. Yanagisawa, Phys. Rev. **C78** (2008) 014308.
232. M. Wiedeking, P. Fallon, A.O. Macchiavelli, J. Gibelin, M.S. Basunia, R.M. Clark, M. Cromaz, M.-A. Deleplanque, S. Gros, H.B. Jeppesen, P.T. Lake, I.-Y. Lee, L.G. Moretto, J. Pavan, L. Phair, and E. Rodriguez-Vietiez, Phys. Rev. Lett. **100** (2008) 152501.
233. Z. Elekes, N. Aoi, Zs. Dombradi, Zs. Fulop, T. Motobayashi, and H. Sakurai, Phys. Rev. **C78** (2008) 027301.
234. S. Shlomo and G. Bertsch, Nucl. Phys. **A243** (1975) 507.
235. K.F. Liu and Nguyen Van Giai, Phys. Lett. **65B** (1976) 23.
236. I. Hamamoto and H. Sagawa, Phys. Rev. **C53** (1996) 1492(R).
237. I. Hamamoto, H. Sagawa, and X.Z. Zhang, Phys. Rev. **C55** (1997) 2361; Nucl. Phys. **A626** (1997) 669; Phys. Rev. **C56** (1997) 3121; Phys. Rev. **C57** (1998) 1064(R); Phys. Rev. **C64** (2001) 024313.
238. T. Nakatsukasa and K. Yabana, Phys. Rev. **C71** (2005) 024301.
239. E. Khan, N. Sandulescu, M. Grasso, and N. Van Giai, Phys. Rev. **C66** (2002) 024309.
240. N. Paar, P. Ring, T. Niksic, and D. Vretenar, Phys. Rev. **C67** (2003) 034312.
241. M. Yamagami and N. Van Giai, Phys. Rev. **C69** (2004) 034301.
242. J. Terasaki, J. Engel, M. Bender, J. Dobaczewski, W. Nazarewicz, and M. Stoitsov, Phys. Rev. **C71** (2005) 034310.
243. K. Yoshida, M. Yamagami, and K. Matsuyanagi, Nucl. Phys. **A779** (2006) 99.
244. S. Peru and H. Goutte, Phys. Rev. **C77** (2008) 044313.
245. K. Yoshida and N. Van Giai, Phys. Rev. **C78** (2008) 064316.

246. C. Losa, A. Pastore, T. Dossing, E. Vigezzi, and R.A. Broglia, *Phys. Rev. C* **81** (2010) 064307.
247. I. Daoutidis and P. Ring, *Phys. Rev. C* **83** (2011) 044303.
248. A. Tamii, I. Poltoratska, P. von Neumann-Cosel, Y. Fujita, T. Adachi, C. A. Bertulani, J. Carter, M. Dozono, H. Fujita, K. Fujita, K. Hatanaka, D. Ishikawa, M. Itoh, T. Kawabata, Y. Kalmykov, A. M. Krumbholz, E. Litvinova, H. Matsubara, K. Nakanishi, R. Neveling, H. Okamura, H.J. Ong, B. Ozel-Tashenov, V.Yu. Ponomarev, A. Richter, B. Rubio, H. Sakaguchi, Y. Sakemi, Y. Sasamoto, Y. Shimbara, Y. Shimizu, F.D. Smit, T. Suzuki, Y. Tameshige, J. Wambach, R. Yamada, M. Yosoi, and J. Zenihiro, *Phys. Rev. Lett.* **107** (2011) 062502.
249. A. Leistenschneider, T. Aumann, K. Boretzky, D. Cortina, J. Cub, U. Datta Pramanik, W. Dostal, Th. W. Elze, H. Emling, H. Geissel, A. Grünschloss, M. Hellstr, R. Holzmann, S. Ilievski, N. Iwasa, M. Kaspar, A. Kleinböhl, J. V. Kratz, R. Kulesa, Y. Leifels, E. Lubkiewicz, G. Münzenberg, P. Reiter, M. Rejmund, C. Scheidenberger, C. Schlegel, H. Simon, J. Stroth, K. Sümmerer, E. Wajda, W. Walus, and S. Wan, *Phys. Rev. Lett.* **86** (2001) 5442.
250. E. Tryggestad, T. Aumann, T. Baumann, D. Bazin, J.R. Beene, Y. Blumenfeld, B.A. Brown, M. Chartier, M.L. Halbert, P. Heckman, J.F. Liang, D.C. Radford, D. Shapira, M. Thoennessen, and R.L. Varner, *Phys. Lett. B* **541** (2002) 52.
251. E. Tryggestad, T. Baumann, P. Heckman, M. Thoennessen, T. Aumann, D. Bazin, Y. Blumenfeld, J.R. Beene, T.A. Lewis, D.C. Radford, D. Shapira, R.L. Varner, M. Chartier, M.L. Halbert, and J.F. Liang, *Phys. Rev. C* **67** (2003) 064309.
252. J. Gibelin, D. Beaumel, T. Motobayashi, Y. Blumenfeld, N. Aoi, H. Baba, Z. Elekes, S. Fortier, N. Frascaria, N. Fukuda, T. Gomi, K. Ishikawa, Y. Kondo, T. Kubo, V. Lima, T. Nakamura, A. Saito, Y. Satou, J.-A. Scarpaci, E. Takeshita, S. Takeuchi, T. Teranishi, Y. Togano, A.M. Vinodkumar, Y. Yanagisawa, and K. Yoshida, *Phys. Rev. Lett.* **101** (2008) 212503.
253. O. Wieland, A. Bracco, F. Camera, G. Benzoni, N. Blasi, S. Brambilla, F.C.L. Crespi, S. Leoni, B. Million, R. Nicolini, A. Maj, P. Bednarczyk, J. Grebosz, M. Kmiecik, W. Meczynski, J. Styczen, T. Aumann, A. Banu, T. Beck, F. Becker, L. Caceres, P. Doornenbal, H. Emling, J. Gerl, H. Geissel, M. Gorska, O. Kavatsyuk, M. Kavatsyuk, I. Kojouharov, N. Kurz, R. Lozeva, N. Saito, T. Saito, H. Schaffner, H.J. Wollersheim, J. Jolie, P. Reiter, N. Warr, G. deAngelis, A. Gadea, D. Napoli, S. Lenzi, S. Lunardi, D. Balabanski, G. LoBianco, C. Petrache, A. Saltarelli, M. Castoldi, A. Zucchiatti, J. Walker, and A. Bürger, *Phys. Rev. Lett.* **102** (2009) 092502.
254. P. Adrich, A. Klimkiewicz, M. Fallot, K. Boretzky, T. Aumann, D. Cortina-Gil, U. Datta Pramanik, Th. W. Elze, H. Emling, H. Geissel, M. Hellström, K.L. Jones, J.V. Kratz, R. Kulesa, Y. Leifels, C. Nociforo, R. Palit, H. Simon, G. Surowka, K. Sümmerer, and W. Walus, *Phys. Rev. Lett.* **95** (2005) 132501.
255. A. Klimkiewicz, N. Paar, P. Adrich, M. Fallot, K. Boretzky, T. Aumann, D. Cortina-Gil, U. Datta Pramanik, Th. W. Elze, H. Emling, H. Geissel, M. Hellström, K.L. Jones, J.V. Kratz, R. Kulesa, C. Nociforo, R. Palit, H. Simon, G. Surowka, K. Sümmerer, D. Vretenar, and W. Walus, *Phys. Rev. C* **76** (2007) 051603(R).
256. T. Hartmann, J. Enders, P. Mohr, K. Vogt, S. Volz, and A. Zilges, *Phys. Rev. Lett.* **85** (2000) 274; T. Hartmann, M. Babilon, S. Kamedzhiev, E. Litvinova, D. Savran, S. Volz, and A. Zilges, *Phys. Rev. Lett.* **93** (2004) 192501.
257. K. Govaert, F. Bauwens, J. Bryssinck, D. De Frenne, E. Jacobs, W. Mondelaers, L. Govor, and V.Yu. Ponomarev, *Phys. Rev. C* **57** (1998) 2229.
258. N. Ryezayeva, T. Hartmann, Y. Kalmykov, H. Lenske, P. von Neumann-Cosel, V.Yu. Ponomarev, A. Richter, A. Shevchenko, S. Volz, and J. Wambach, *Phys. Rev. Lett.*

- 89** (2002) 272502.
259. J. Enders, P. von Brentano, J. Eberth, A. Fitzler, C. Fransen, R.-D. Herzberg, H. Kaiser, L. Käubler, P. von Neumann-Cosel, N. Pietralla, V.Yu. Ponomarev, A. Richter, R. Schwengner, I. Wiedenhöver, Nucl. Phys. **A724** (2003) 243.
260. R.-D. Herzberg, P. von Brentano, J. Eberth, J. Enders, R. Fischer, N. Huxel, T. Klemme, P. von Neumann-Cosel, N. Nicolay, N. Pietralla, V.Yu. Ponomarev, J. Reif, A. Richter, C. Schlegel, R. Schwengner, S. Skoda, H.G. Thomas, I. Wiedenhöver, G. Winter, and A. Zilges, Phys. Lett. **B390** (1997) 49.
261. R.-D. Herzberg, C. Fransen, P. von Brentano, J. Eberth, J. Enders, A. Fitzler, L. Käubler, H. Kaiser, P. von Neumann-Cosel, N. Pietralla, V.Yu. Ponomarev, H. Prade, A. Richter, H. Schnare, R. Schwengner, S. Skoda, H.G. Thomas, H. Tiesler, D. Weisshaar, and I. Wiedenhöver, Phys. Rev. **C60** (1999) 051307.
262. A. Zilges, S. Volz, M. Babilon, T. Hartmann, P. Mohr, and K. Vogt, Phys. Lett. **B542** (2002) 43.
263. S. Volz, N. Tsoneva, M. Babilon, M. Elvers, J. Hasper, R.-D. Herzberg, H. Lenske, K. Lindenberg, D. Savran, and A. Zilges, Nucl. Phys. **A779** (2006) 1.
264. D. Savran, M. Babilon, A. M. van den Berg, M. N. Harakeh, J. Hasper, A. Matic, H. J. Wörtche, and A. Zilges, Phys. Rev. Lett. **97** (2006) 172502.
265. D. Savran, M. Fritzsche, J. Hasper, K. Lindenberg, S. Müller, V.Yu. Ponomarev, K. Sonnabend, and A. Zilges, Phys. Rev. Lett. **100** (2008) 232501.
266. A.P. Tonchev, S.L. Hammond, J.H. Kelley, E. Kwan, H. Lenske, G. Rusev, W. Tornow, and N. Tsoneva, Phys. Rev. Lett. **104** (2010) 072501.
267. S. Goriely, E. Khan, and M. Samyn, Nucl. Phys. **A739** (2004) 331.
268. J. Piekarewicz, Phys. Rev. **C73** (2006) 044325.
269. T. Inakura, T. Nakatsukasa, and K. Yabana, Phys. Rev. **C84** (2011) 021302(R).
270. P.-G. Reinhard and W. Nazarewicz, Phys. Rev. **C81** (2010) 051303(R).
271. S. Yoshida and H. Sagawa, Phys. Rev. **C69** (2004) 024318; Phys. Rev. **C73** (2006) 044320.
272. W. Nazarewicz and R.F. Casten, Nucl. Phys. **A682** (2001) 295c.